IEEE Access
Multidisciplinary ⋮ Rapid Review ⋮ Open Access Journal

Received 9 June 2022, accepted 3 July 2022, date of publication 25 July 2022, date of current version 4 August 2022.

Digital Object Identifier 10.1109/ACCESS.2022.3193490

RESEARCH ARTICLE

Network Synchronization Revisited: Time Delays in Mutually Coupled Oscillators

LUCAS WETZEL[1], DIMITRIOS PROUSALIS[1], RABIA FATIMA RIAZ[3], CHRISTIAN HOYER[3], NIKO JORAM[3], JOHANNES FRITZSCHE[2], FRANK ELLINGER[3,4], (Senior Member, IEEE), AND FRANK JÜLICHER[1]

[1]Max Planck Institute for the Physics of Complex Systems, 01187 Dresden, Germany
[2]Kazoosh, 01099 Dresden, Germany
[3]Chair for Circuit Design and Network Theory, Technische Universität Dresden, 01069 Dresden, Germany
[4]Centre for Tactile Internet With Human-in-the-Loop (CeTI), Technische Universität Dresden, 01069 Dresden, Germany

Corresponding author: Lucas Wetzel (lwetzel@pks.mpg.de)

This work was supported by the Federal Ministry of Education and Research (BMBF) under Grant 03VP06431.

ABSTRACT Coordinated and efficient operation in large, complex systems requires the synchronization of the rhythms of spatially distributed components. Such systems are the basis for critical infrastructure such as satellite navigation, mobile communications, and services like the precision time protocol and Universal Coordinated Time. Different concepts for the synchronization of oscillator networks have been proposed, in particular mutual synchronization without and hierarchical synchronization from a reference clock. Established network synchronization models in electrical engineering address the role of inevitable cross-coupling time delays for network synchronization. Mutual synchronization has been studied using linear approximations of the coupling functions of these models. We review previous work and present a general model in which we study synchronization taking into account nonlinearities and finite time delays. As a result, dynamical phenomena in networks of coupled electronic oscillators induced by time delays, such as the multistability and stabilization of synchronized states can be predicted and observed. We study the linear stability of nonlinear states and predict for which system parameters synchronized states can be stable. We use these results to discuss the implementation of mutual synchronization for complex system architectures. A key finding is that mutual synchronization can result in stable in- and anti-phase synchronized states in the presence of large time delays. We provide the condition for which such synchronized states are guaranteed to be stable.

INDEX TERMS Synchronization, delay effects, systems engineering and theory, control theory, phase locked loops, mutual coupling.

I. INTRODUCTION

Network synchronization provides the basis for concerted operation of natural and engineered systems [1]–[5]. It refers to the concepts to synchronize the nodes of a network, i.e., mutual synchronization, hierarchical entrainment and the plesiosynchronous ansatz [6]. The hierarchical approach is the basis for time distribution services like the Network- and Precision Time Protocol. The demand for timing services available over large geographical scales was initiated with the onset of railway transportation and telegraph systems [7]. With the introduction of pulse-code modulation in communication networks during the 1950s, efforts towards the development of mathematical frameworks to study synchronization were made [7]–[9]. The speed of light sets an upper limit for signal transmission velocities. Therefore cross-coupling time delays between a networks' nodes are unavoidable [10], [11]. Such time delays affect the dynamics of synchronization in networks of coupled oscillators. Particularly the setup of complex spatially distributed systems operating at high frequencies has generated novel challenges to synchronization solutions. In hierarchical synchronization, i.e., the entrainment of oscillators by a reference clock, time delays cause phase differences in the networks' clocking

The associate editor coordinating the review of this manuscript and approving it for publication was Wonhee Kim.

signals. Delay-compensation techniques can address the presence of such cross-coupling time delays. However, they become uneconomic or difficult to achieve as the spatial dimension, complexity or frequency of operation of a system increases [12]. This is the case in, e.g., localization services, data processing on global scale, radio astronomy, and mobile communication systems [13], [14]. Synchronization solutions that scale with system size are needed as systems grow larger and tend to be more distributed. In non-hierarchical mutual synchronization time delays do not introduce phase-differences, instead they affect the frequency and stability of synchronized states. The precision of mutual synchronization has also been shown to scale advantageously with system size [6]. It is suggested to become increasingly relevant due to its robustness against time-delayed cross-coupling [15], [16], [18], [19]. In this approach, neither delay compensation nor centralized control is necessary. It can serve as the backbone for large, distributed systems, e.g., meshed and ad-hoc network structures [20] that play an important role in modern society.

The seminal contributions on *Network Synchronization* in the late 1950s addressed the effects of the unavoidable cross-coupling time delay and oscillators' signal processing [7], [8], [21]–[23]. These were reviewed in Lindsey *et al.* [6] which points out that *"the analysis of the mathematical model in its most general form ... is a difficult problem"*. These works studied the properties of synchronized states and their stability after linearization of nonlinear coupling functions. The results well approximate the properties of synchronized states for time delays of the order of the oscillation period. Recent advances in dynamical systems theory and the field of delay integro-differential equations has revealed new phenomena like multistability and parameter-heterogeneity induced stabilization of synchronized states [24]–[26].

In this paper we address synchronization dynamics in the presence of considerable cross-coupling time delays for any static network topology. To provide a full picture we review and generalize the mathematical models previously discussed by, e.g., Lindsey *et al.* [6] and Pollakis *et al.* [24]. In Sec. II we generalize these models to include more general coupling functions that describe feedback-path time delays, as well as effects of inverters and frequency dividers. We discuss the dynamics of a free-running phase-locked loop and show how the intrinsic frequency depends on the internal dynamics of the PLL. Using tools from delay dynamical systems theory we then analyze network synchronization with the general nonlinear model [27]–[36]. The analysis in Sec. III-A reveals that multiple synchronized states with different properties can emerge for the same oscillator and network parameters. Taking into account the nonlinearity of the coupling function, we derive in Sec. III-B and III-C expressions for the loop gains and transfer functions of individual oscillators and networks of oscillators. These depend not only on the circuit properties of the oscillator itself but also on those of the network and the synchronized states that can exist therein. We use the loop gains and transfer functions to analyze the stability of synchronized states beyond the critical point, i.e., beyond the point where the system is marginally stable. Using these we present explicit expressions for the properties of the perturbation response, e.g., its characteristic time scale. This enables a precise differentiation of the stability and multistability of synchronized states, such as in-phase, anti-phase, and so-called twist-states. We define the delay-margin as the value of the cross-coupling time delay for which a synchronized state becomes unstable for the first time. Using the properties of the network topology, the steady state loop gain and the loop filter cut-off frequencies, we present a stability condition for the linear stability of synchronized states. If this condition is fulfilled, it implies that synchronized states with constant frequency are stable for any value of the cross-coupling time delay. We then show that mutual synchronization is possible at time delays hundreds of thousand times larger than the oscillation period, see Sec. III-C. We address one of the major challenges of mutual synchronization – its complexity of implementation – an issue raised in Ref. [6], see Sec. II Table 1 therein. The theoretical results of sections III-A and III-B are then used to compare entrainment to mutual synchronization in Sec. IV. A time-domain simulation of the dynamics of a network of 64 mutually coupled oscillators demonstrates that mutual synchronization is feasible in the presence of considerable time delays, see Sec. IV-C. We then discuss how network topology and node parameters can guide and optimize synchronization in Sec. V. Such guidance and optimization can be realized using inverters, tuning voltages, frequency dividers, tuned component heterogeneity and custom fit oscillator design. Hence, this work provides all necessary theoretical tools to guide the systems design of complex oscillator networks in the presence of significant time delays and inert oscillator response.

II. NETWORK SYNCHRONIZATION THEORY

Here we briefly review, generalize and extend the theoretical framework within which network synchronization can be studied. The analysis presented in this work is based on tools from dynamical systems theory and delay integro-differential equations (DIDEs) [27], [28], [31]. The results obtained within these theoretical frameworks are then discussed from a control theory perspective. This work introduces network synchronization theory also valid for cross-coupling time delays larger than the period of the oscillations. Therefore, we first discuss the differences between different definitions of synchronization. Then we establish how the internal dynamics of an oscillator relate to the notion of its intrinsic frequency, defining the autonomous oscillator. It is the basis for studying synchronization in the framework of Kuramoto-type oscillators [37], [38]. This work then studies networks of coupled oscillators that are solely characterized by the phases of their oscillations. The amplitudes are considered to be constant and no interactions between the amplitudes and phases are considered. Such phase models

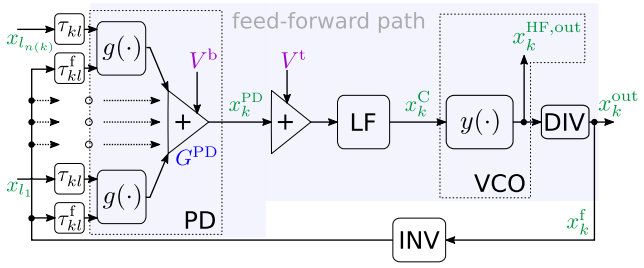

FIGURE 1. Sketch of a phase-locked loop (PLL) node indexed by k with multiple inputs $x_{l_{n(k)}}$ and calibration voltages $\{V^{\mathrm{b}}, V^{\mathrm{t}}\}$ to control internal properties.

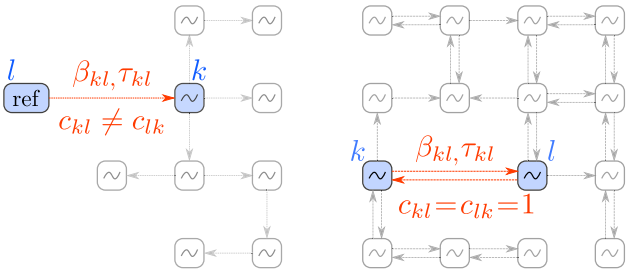

FIGURE 2. (left) Hierarchical clock tree network structure with reference oscillator. (right) Mutual coupling network structure without a reference oscillator.

can be obtained from the dynamical equations of the signals of, e.g., electronic oscillators, using phase reduction methods [5], [39].

A. DEFINITION OF TIME, FREQUENCY AND PHASE SYNCHRONIZATION

In order to discuss the existence of synchronized states and their properties we here define the necessary concepts. *Frequency synchronization* denotes the process during which a set of oscillators adjust their instantaneous frequencies such that these become equal asymptotically. As a result the oscillators' phases are locked [5]. The phase $\phi(t) \in [0,\ 2\pi)$ of an oscillation linearly maps the progression within one period. Hence, for cross-coupling time delays larger than a period, phase synchronization does not imply time synchronization. *Phase synchronization* relates to frequency synchronization with specific constant phase relations, such as 0 or π for so-called in- and anti-phase synchronized states. In physics, *time* is defined by what a clock measures [40]. Therefore, a local time can be derived from a counter that counts the cycles of the periodic output of an oscillator. Consequently, *time synchronization* denotes the synchronization of the time-measures derived from a set of clocks. That means that after phase-synchronization has been achieved, the counters need to be reset accordingly using Einstein synchronization [41].

B. GENERAL DYNAMICAL SYSTEMS MODEL OF A PHASE-LOCKED LOOP

The nodes considered here consist of a phase-detector (PD), loop-filter (LF), signal inverter (INV), divider (DIV), and voltage controlled oscillator (VCO) that form a feedback loop system. This resembles a phase-locked loop (PLL), see Fig. 1, widely used in electronic systems [42]. The PD detects the phase relations between external signals $x_l^{\mathrm{ext}}(t-\tau)$ indexed by $l \in \mathbb{N}$ and an internal feedback signal $x^{\mathrm{f}}(t-\tau^f)$. The symbols τ and τ^f denote the cross-coupling and feedback time delays, respectively. The PD output signal is a function of these input signals and can optionally be shifted by a voltage V^{b}

$$x^{\mathrm{PD}}(t) = G^{\mathrm{PD}}\left(V^{\mathrm{b}} + \frac{1}{n}\sum_{l=1}^{n} g\left(x_l^{\mathrm{ext}}(t-\tau),\ x^{\mathrm{f}}(t-\tau^f)\right)\right), \tag{1}$$

where $g(\cdot)$ can be a nonlinear function of the incoming signals depending on the type of PD and G^{PD} denotes the gain of the adder. The PD signal is then filtered and a tuning voltage V^{t} can be added to yield the control signal

$$x^{\mathrm{c}}(t) = V^{\mathrm{t}} + \int_0^\infty \mathrm{d}u\, p(u)\, x^{\mathrm{PD}}(t-u), \tag{2}$$

where $p(u)$ denotes the impulse response of the LF. The voltages V^{b} and V^{t} can be used to change the operation point of the PLL, see Appendix VI. The instantaneous frequency of the VCO is controlled by $x^{\mathrm{c}}(t)$

$$\dot{\phi}^{\mathrm{VCO}}(t) = y(x^{\mathrm{c}}(t)). \tag{3}$$

The functional form of $y(\cdot)$ depends on the architecture of the VCO and can be a nonlinear function of its input voltage. Linearizing this function around the intrinsic frequency ω_0 of the VCO, its instantaneous output frequency can be obtained

$$\dot{\phi}^{\mathrm{VCO}}(t) = \omega_0 + K^{\mathrm{VCO}}\, x^{\mathrm{c}}(t), \tag{4}$$

where K^{VCO} denotes its sensitivity close to the operation point, see Appendix VI. From this the instantaneous angular PLL frequency $\dot{\phi}_k(t)$ when closing the feedback loop can be studied

$$\begin{aligned}\dot{\phi}(t) &= \omega_0 + K^{\mathrm{VCO}} \int_0^\infty \mathrm{d}u\, p(u)\, \left(V^{\mathrm{s}} + G^{\mathrm{PD}} g(0,\ x^{\mathrm{f}}(t-u-\tau^f))\right) \\ &= \omega. \end{aligned} \tag{5}$$

Note that we defined $V^{\mathrm{s}} = V^{\mathrm{t}} + G^{\mathrm{PD}} V^{\mathrm{b}}$, where V^{t} can tune the intrinsic PLL frequency independently of G^{PD}. As a result, if there are no external input signals, the dynamics of the PD and V^{t} determine the intrinsic PLL frequency ω. It can be different from the intrinsic frequency ω_0 of the VCO, e.g., as can be the case for XOR PD elements. Hence, knowledge of the internal dynamics allows to abstract a PLL as an autonomous oscillator characterized by effective parameters, e.g., intrinsic frequency and duty cycle.

The case of an XOR PD is discussed in Appendix VI as it has important implications for the architecture design process of the PD part of a digital PLL (DPLL). In mutual synchronization systems design the PLL component's gain

characteristics can be a useful control parameter. Hence, the PD should be designed such that the intrinsic PLL frequency is independent of those gains. This can be achieved by, e.g., using V^{b} to shift the mean output voltage of the PD to zero.

C. SYNCHRONIZED STATES IN NETWORKS OF DELAY-COUPLED PLLs

We now discuss synchronization dynamics in networks of heterogeneous PLLs in the presence of cross-coupling time delays for clock tree and mutual coupling architectures, see Fig. 2. In the following, implementation related nonlinearities are treated in the small signal limit. We focus on the nonlinearities in the coupling. If necessary, additional nonlinearities in, e.g., the VCO's response can also be taken into account [43]. For a network of N coupled oscillators we find the dynamics of the PLLs' instantaneous frequencies

$$\dot{\phi}_k(t) = \omega_k + \frac{K_k}{n(k)} \sum_{l=1}^{N} c_{kl} \int_0^\infty \mathrm{d}u\, p_k(u)\, h\left(\frac{\delta\phi_{kl}(t,\, u,\, \tau)}{v} + \phi_k^{\mathrm{INV}} \right), \tag{6}$$

where $k = 1, \ldots, N$ indexes the N PLLs in the network, $\omega_k = \omega_0 + K_k^{\mathrm{VCO}} V^{\mathrm{t}} + \xi\, G_k^{\mathrm{TOT}} K_k^{\mathrm{VCO}} V^{\mathrm{b}}/2$ denotes the intrinsic frequency of PLL k with $\xi = 0$ for multiplier and $\xi = 1$ for XOR PDs and G_k^{TOT} the product of all gains in the feed-forward path, $K_k = G_k^{\mathrm{TOT}} K_k^{\mathrm{VCO}}/2$ the coupling strength, $n(k)$ the number of input signals, c_{kl} the components of the network's adjacency matrix being either one if there is a connection from PLL l to k or zero otherwise, $p_k(u)$ the impulse response function of the loop filter, $\delta\phi_{kl}(t,\, u,\, \tau) = \phi_l(t - u - \tau_{kl}) - \phi_k(t - u - \tau_{kl}^f)$ the phase difference between the PD input signals' phases, τ_{kl} the cross-coupling time delay from node l to k, τ_{kl}^{f} the feedback path time delay within node k towards an input l, v the divisor of the frequency divider, and ϕ_k^{INV} a phase-shift induced by an inverter element taking values 0 (deactivated) or π (active). Based on $p_k(u)$ a LF cut-off frequency ω_k^{c} can be defined. The coupling function $h(\cdot)$ is 2π-periodic with a normalized peak-to-peak amplitude equal to 2 and can be calculated from Eq. (1) in the case where the LF ideally filters the PD signal [24], [39]. That means dropping from the Fourier representation of $g(\cdot)$ all high frequency contributions. For digital PLLs with XOR PD the coupling function then is a triangular function, for analog PLLs a cosine function of the phase differences between the feedback and input signals. Hence in many cases this dynamical model for networks of delay-coupled PLLs reduces to a generalized Kuramoto phase-oscillator model [37]. In Laplace space the coupling function is also referred to as the phase error transfer function.

III. NONLINEAR CONTROL THEORY FOR LARGE PLL NETWORKS WITH TIME-DELAYED COUPLING

We now study synchronization in complex networks of delay-coupled oscillators using the tools from dynamical systems theory. This analysis will then be connected to well known concepts from control theory using its terminology and figures of merit [46]–[49]. Specifically, we extend the concept of the loop gain and the transfer functions and introduce a definition of the delay margin. Using these we study linear stability and the stability at the critical point. As a result we present a novel condition for the stability of synchronized states. The focus will be on the dynamics of networks of mutually delay-coupled PLLs, while treating each individual PLL as an autonomous oscillator.

A. EXISTENCE AND PROPERTIES OF SYNCHRONIZED STATES

In time-domain the ansatz for frequency-synchronized states with global frequency Ω subject to a small ($\epsilon \ll 1$) phase perturbation $q_k(t)$ in a network composed of N oscillators is

$$\phi_k(t) = \Omega t + \beta_k + \epsilon q_k(t), \tag{7}$$

where β_k denotes the phase-offset of oscillator k with respect to a reference phase. Plugging the ansatz into the set of Eqs. (6), the properties of synchronized states and their stability can be calculated. Expansion of the coupling function and sorting by orders of ϵ we obtain a set of N coupled nonlinear equations from which the frequency Ω of the synchronized state and the $N-1$ phase relations β_{kl} between the oscillators can be computed

$$\Omega = \omega_k + \frac{K_k}{n(k)} \sum_{l=1}^{N} c_{kl}\, h\left(\frac{-\Omega\tau_{kl}^{\mathrm{e}} - \beta_{kl}}{v} + \phi^{\mathrm{INV}} \right), \tag{8}$$

where $\tau_{kl}^{\mathrm{e}} = \tau_{kl} - \tau_{kl}^f$ and $\beta_{kl} = \beta_k - \beta_l$. This characterizes the properties of existing frequency and phase synchronized states. Each term in the sum over all inputs l to a PLL k with $c_{kl} \neq 0$ represents a contribution to the VCO's control signal in a synchronized state. The argument of the coupling function $h(\cdot)$ is composed of the actual instantaneous phase-relation β_{kl} between two oscillators and a contribution $-\Omega\tau_{kl}^{\mathrm{e}}$ related to the delayed coupling. Hence, the arguments of $h(\cdot)$ represent the phase relations seen by the PD of PLL k for each of its inputs from PLLs l in a synchronized state. Note that the set of Eqs. (8) is implicit in Ω. As a result multistability of synchronized solutions can exist for the case of mutual synchronization. Multistability occurs when multiple synchronized states with difference frequencies and phase relations can exist for the same set of parameters. In the case of entrainment by a reference oscillator, i.e. $\Omega = \omega_{\mathrm{ref}}$, the frequency becomes a parameter in the set of Eqs. (8). Then the phase relations β_{kl} in the clock tree can be calculated. Note that the results presented in this work hold for constant cross-coupling time delay. When the time delay changes adiabatically, i.e., all oscillators remain phase-locked while τ_{kl}^{e}

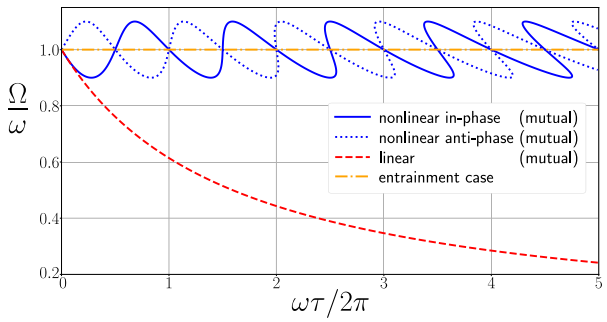

FIGURE 3. Frequencies of synchronized states vs the cross-coupling time delay. Results shown for a system of $N = 2$ coupled identical oscillators with sinusoidal coupling function, for the entrainment case and the mutual coupling case. The LF is modeled as a single RC element using the Γ-distribution with shape parameter $a = 1$ and integration time $\tau^c = (\omega^c)^{-1}$. PLL parameters are $\omega = 2\pi \cdot 1.0$ Hz (intrinsic frequency), $K = 2\pi \cdot 0.1$ Hz/V (coupling strength), $\omega^c = 2\pi \cdot 0.14$ Hz (LF cut-off frequency), $v = 1$ (divisor) and for entrainment $\omega_{\text{ref}} = 2\pi \cdot 1.0$ Hz (reference frequency).

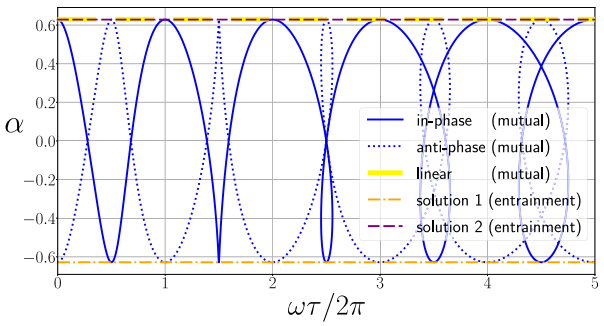

FIGURE 4. State-dependent loop gain vs the cross-coupling time delay in multiples of the period of the intrinsic PLL frequency. Due to state-dependence different loop gain values are obtained for the same system parameters (specified in Fig. 3) associated to in- and anti-phase synchronization.

changes, the frequency of phase-locked synchronized states will change as shown by the curves in, e.g., Fig. 3 and [43]. For non-adiabatically changing parameters an analysis based on time dependent solutions is required.

The results shown above compare as follows to those presented in [6]. There the properties of synchronized states are calculated after linearizing the set of dynamical Eqs. (6) making an ansatz for frequency synchronized states as shown in Eq. (7), see Sec. III-E in [6]. This leads to a qualitatively different result for the frequency of in-phase synchronized states with the following structure

$$\Omega = \frac{\frac{\omega_k\, v}{K_k}}{\frac{v}{K_k} + \frac{1}{n(k)} \sum_l c_{kl}\, \tau_{kl}}, \tag{9}$$

see Sec. VI Table 3 in [6]. This is only valid for small cross-coupling time delays, compare Fig. 3. It depicts solutions to Eq. (8) and Eq. (9) for an example system of $N = 2$ mutually delay-coupled PLLs with unit intrinsic frequencies as a function of the cross-coupling time delay. Apparently, key phenomena of mutual synchronization in the presence of cross-coupling time delays, such as the multistability and their frequencies, can only be studied and analyzed in the set of the nonlinear Eqs. (6). Additionally, the entrainment case is plotted for comparison. It has two solutions to β_{12}, see Fig. 12. Note that PLL parameters, used in all figures of the manuscript, are rescaled to an intrinsic PLL frequency of 1 Hz for simplicity. The results however hold for any frequency regime.

B. NETWORK STABILITY AND THE ROLE OF STATE-DEPENDENT LOOP GAIN

In this section we study the stability of the synchronized states discussed in the previous section with respect to small perturbations when $\tau^f_{kl} = \tau^f_k$. The technical details of the derivation of the equations discussed here can be found in Appendix VI. In Laplace space the output phase error $q_k(\lambda)$, with $\lambda = \sigma + j\gamma$, of a PLL k depends on all phase errors received from external inputs l in the network via the following general expression for the perturbation dynamics

$$q_k(\lambda) = \frac{\sum_{l=1}^{N} \tilde{c}_{kl}\, H^{\text{FF}}_{kl}(\lambda)\, e^{-\lambda\tau_{kl}}\, q_l(\lambda)}{1 + e^{-\lambda\tau^f_k} \sum_{l'=1}^{N} \tilde{c}_{kl'}\, H^{\text{FF}}_{kl'}(\lambda)}\,. \tag{10}$$

We defined $\tilde{c}_{kl} = c_{kl}/n(k)$ and introduced $H^{\text{FF}}_{kl}(\lambda)$ as the *feed-forward transfer function* for each input l to a PLL k. It is equal to the product of the gains of the components in the feed-forward path

$$H^{\text{FF}}_{kl}(\lambda) = \alpha_{kl} \frac{\hat{p}_k(\lambda)}{\lambda}, \tag{11}$$

where the

$$\alpha_{kl} = \frac{K_k}{v}\, h'\left(\frac{-\Omega\tau^{\text{e}}_{kl} - \beta_{kl}}{v} + \phi^{\text{INV}}_k\right), \tag{12}$$

are the steady-state loop gains for each individual external input path l of PLL k, $h'(\cdot)$ denotes the derivative of the coupling function with respect to its argument, and $\hat{p}_k(\lambda)$ is the Laplace transformed impulse response function of the LF. Furthermore, σ and γ in the definition of the Laplace variable λ denote a rate and frequency of the perturbation response dynamics, respectively.

Analyzing Eq. (10) for a single PLL k allows to study whether a PLL can be stably entrained by the external input signals, either from a reference oscillator or a network of PLLs. We call that *nodal stability*. It becomes apparent that the nodal stability of each PLL in the network depends on the properties of all its feed-forward paths $H^{\text{FF}}_{kl}(\lambda)$. Furthermore, the *steady state loop gain* of a PLL k is $\alpha_k = \sum_l \tilde{c}_{kl}\alpha_{kl}$, hence the mean over all α_{kl} for which $c_{kl} \neq 0$. It depends explicitly on the properties of the synchronized state itself whose stability is under investigation and not only on the internal PLL and network properties. Consequently, each PLL's steady state loop gain is state-dependent and can take positive and negative values, see Fig. 4. In the linear model [6] the loop gain is constant and equal to the yellow dashed line. In the entrainment case the loop gain depends on the steady state phase relations between the reference and the PLL [50]. These compensate for the time delay dependence and render the loop gain constant, see Fig. 4. For mutual

synchronization the loop gain depends on the frequency of a synchronized state and hence on the time delays in the network. Another important parameter is the *loop bandwidth*, e.g., the equivalent noise bandwidth and the 3-dB bandwidth of the closed-loop transfer function. As Gardner states [51], the steady state loop gain is a relevant parameter for the analysis of the dynamic behavior of a PLL, including its loop bandwidth. Hence, loop bandwidths that depend on the loop gain also become state dependent. In Sec. III-C we show how gain, phase and delay margins can be obtained from the state dependent loop gain and transfer functions. Now we will discuss how the dynamic behavior can be quantified using perturbation response rates from linear stability analysis.

Due to the heterogeneity of the oscillators' intrinsic frequencies, coupling strengths, impulse response functions and time delays in the networks considered here, it is not straightforward to obtain a transfer function for the network from the set of Eqs. (10). Here we show how stability can be studied analyzing the matrix form. Only when all N oscillators and cross-coupling time delays are identical, or for $N = 2$, the set of equations collapses to a single transfer function, for details see Sec. IV-B and Appendix VI. The stability of synchronized states in networks of delay-coupled PLLs can be studied analyzing all solutions λ to the set of the N coupled Eqs. (10). In matrix form $\vartheta\,\mathbf{q} = \mathbf{G}\cdot\mathbf{q}$, where $\vartheta = 1$ denotes the eigenvalue, and $\mathbf{q} = (q_1, q_2, \ldots, q_N)$ the eigenvectors of $\mathbf{G}$. The matrix elements are given by

$$G_{kl} = \tilde{c}_{kl}\,\alpha_{kl} e^{-\lambda\tau^{e}_{kl}} \left(\frac{\lambda}{\hat{p}_k(\lambda) e^{-\lambda\tau^{f}_{k}}} + \sum_{l'=1}^{N} \tilde{c}_{kl'}\alpha_{kl'} \right)^{-1}. \quad (13)$$

Arbitrary perturbation vectors can be represented by the $\mathbf{q}$ for diagonalizable $\mathbf{G}$. Given the G_{kl} and evaluating

$$\det(\mathbf{G} - \mathbf{I}) = 0, \quad (14)$$

yields the characteristic equation for the linear stability of synchronized states in networks of delay-coupled heterogeneous PLLs [26]. Eq. (14) has a discrete infinite set of solutions λ. We denote with λ_0 the one with the largest real part σ_0 that dominates a systems perturbation response close to synchronized states. If $\sigma_0 < 0$ small perturbations decay and the synchronized state is linearly stable and robust to small perturbations. For $\sigma_0 > 0$ it is linearly unstable and perturbations grow, see white regimes in Fig. 6. We call σ_0 the perturbation response rate which is proportional to the time scale of synchronization. From this a characteristic perturbation response time $t^r = -\sigma_0^{-1}$ for which perturbations have decayed to $1/e$ of their initial value can be calculated. The critical point $\sigma_0 = 0$ represents the marginal stable case in which perturbations neither grow nor decay. The imaginary part γ_0 of λ_0 denotes a frequency associated to the perturbation dynamics. If $\gamma_0 = 0$ the perturbation response is overdamped, while for $\gamma_0 > 0$ it is underdamped, see Fig. 6. All other solutions $\lambda \neq \lambda_0$ relate to other faster decaying perturbation modes in the network.

For identical PLLs and cross-coupling time delays, $G_{kl}(\lambda) = G(\lambda)$, the perturbation modes defined by the network topology decouple from the properties of the nodes. Hence, Eq. (14) simplifies to $G^{-1}(\lambda)\,\vartheta\,\mathbf{q} = \mathbf{C}\cdot\mathbf{q}$. We then identify

$$e^{\lambda\tau^{e}} \left(\frac{e^{\lambda\tau^{f}}}{H^{\mathrm{FF}}(\lambda)} + 1 \right) = \zeta, \quad (15)$$

with $\zeta\cdot\mathbf{q} = \mathbf{C}\cdot\mathbf{q}$, where the $\zeta = |\zeta| e^{i\Psi} \in \mathbb{C}$ are the eigenvalues of the adjacency matrix $\mathbf{C}$ that represents the network's coupling topology with components c_{kl} [24], [39].

We note here, that in [52] a general necessary and sufficient condition for the stability of synchronized states in a model of delay-coupled phase-oscillators has been derived. This model is different from the one given by the set of Eqs. (6) as it does not include a LF. They show that if $\alpha > 0 \leftrightarrows \mathrm{Re}(\lambda_0) < 0$, i.e., small perturbations to the synchronized state decay if the steady state loop gain is positive. Their result holds for identical oscillators and cross-coupling time delays and any

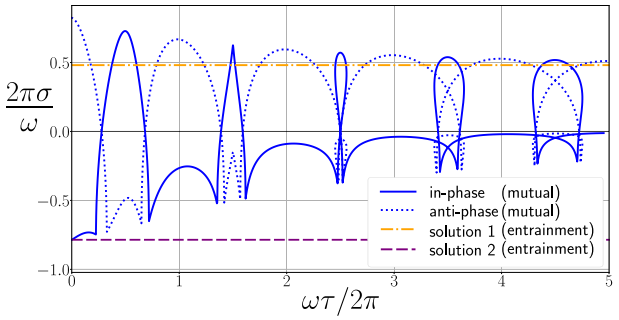

FIGURE 5. Perturbation response rate part $\sigma = \mathrm{Re}(\lambda)$ vs the cross-coupling time delay τ in multiples of the intrinsic period of the PLL $T = 2\pi/\omega$. Rescaling σ with T we show whether initial perturbations decays slower ($\sigma T > -1$) than a period or faster ($\sigma T < -1$). Note that there is so called multistability within either in- or anti-phase synchronized states in regimes where multiple solutions exist for the same argument. For system parameters see Fig. 3.

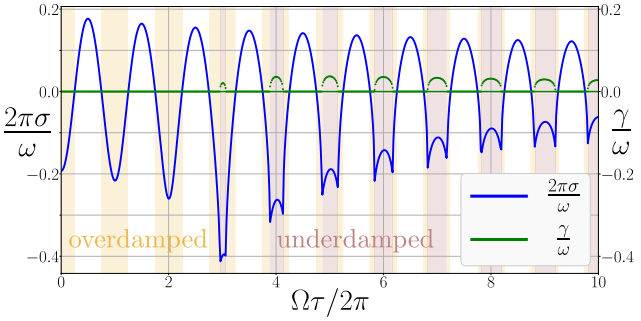

FIGURE 6. Perturbation response rate σ_0 and frequency γ_0 plotted as a function of the cross-coupling time delay τ. Over- and underdamped perturbation response regimes are shown. The $N = 2$ PLLs' parameters are $\omega = 2\pi \cdot 1.0$ Hz, $K = 2\pi \cdot 0.015$ Hz/V, $\omega^{c} = 2\pi \cdot 1.46$ Hz, $\nu = 1$ and $h(x) = \sin(x)$. Note that here the multistability is not visible as in, e.g. Fig. 5, as we plot against the phase difference with respect to the synchronized state with frequency Ω.

network topology in which all oscillators have the same number of inputs. In terms of mutual synchronization the absence of a loop filter implies that there can be stable synchronization for any value of the cross-coupling time delay if no dynamical noise is considered. However, introducing a LF to the PLL affects its response time. This allows for additional control of the PLLs properties and regulates the quality of the oscillations in the presence of noise [53], [54]. As a loop filter is included in the oscillator model, the order of the polynomial of the characteristic equation increases by the order of the LF. As a result this stability condition is not valid anymore and becomes sufficient only, $\alpha < 0 \rightarrow \mathrm{Re}(\lambda_0) > 0$. In terms of the steady state loop gain, $\alpha < 0$ indicates that the synchronized state represented in the argument of $h'(\cdot)$ is unstable, see Figs. 5 and 4. In this case perturbations to the synchronized states are amplified. For $\alpha > 0$ new types of instabilities can be studied in the model that includes the LF, see the set of Eqs. (6). These instabilities lead to states with highly correlated but time-dependent frequencies that do not exist in first order Kuramoto oscillator models [39], or chaos [26]. They can arise in regimes with underdamped perturbation response, see Fig. 10. Choices of the PLLs' loop gain, network topology and LF cut-off frequency ω^c for which these instabilities cannot exist and synchronized states are robust against small perturbations are given by the following general sufficient condition:

$$\frac{\omega^c}{2|\alpha|} > 1 - \sqrt{1 - |\zeta_0|^2}, \tag{16}$$

where ζ_0 denotes the eigenvalue of the adjacency matrix $\mathbf{C}$ with the largest magnitude, see Fig. 7. This extends the previously known stability condition $K/\omega^c < 1/2$, see [6], [55], to include the properties of the network topology and the properties of the synchronized state. This result holds for networks of identical PLLs with first order LFs. Hence, adding the loop filter to the dynamical phase model provides a more realistic understanding of the synchronization dynamics in PLL networks.

C. NETWORK STABILITY AT THE CRITICAL POINT: STATE-DEPENDENCE OF THE PERTURBATION RESPONSE, AND THE PHASE AND GAIN MARGIN

In the previous section we studied the linear stability of synchronized states computing the complex roots λ of the characteristic Eq. (14). Here we discuss how taking into account the full nonlinearity of the set of model Eqs. (6) affects the phase, gain and delay margin in network synchronization situations. That means we study the properties of individual PLLs that are part of a network over which a specific synchronized state has formed. In control theory these concept are related to studying the dynamics of a system close to the critical point, i.e., for $\sigma = 0$ and hence $\lambda_c = j\gamma_c$. This simplifies the analysis of characteristic equations and yields important information about a system's gain, phase and delay margins [34], [56]–[58].

Taking into account the nonlinearities in the set of Eqs. (6) we find for the gain margin of a single PLL k with $n(k)$ inputs according to its definition:

$$m_g(\gamma_c^{\mathrm{p}}) = 1 - \left| \sqrt{\mathrm{Re}\left(H_k^{\mathrm{OL}}(j\gamma_c^{\mathrm{p}})\right)^2 + \mathrm{Im}\left(H_k^{\mathrm{OL}}(j\gamma_c^{\mathrm{p}})\right)^2} \right|, \tag{17}$$

where γ_c^{p} is the so-called phase crossover frequency. With $H_k^{\mathrm{OL}}(j\gamma_c)$ we denote the open-loop transfer function of PLL k, the normalized sum over all feed-forward transfer functions $H_{kl}^{\mathrm{FF}}(j\gamma_c)$ multiplied with the feedback-delay term

$$H_k^{\mathrm{OL}}(j\gamma_c) = e^{-j\gamma_c \tau_k^f} \sum_{l=1}^{N} \tilde{c}_{kl} \alpha_{kl} \frac{\hat{p}_k(j\gamma_c)}{j\gamma_c}, \tag{18}$$

where α_{kl} denotes the steady-state loop gain for each individual external input path which is a nonlinear function of the properties of synchronized states, see Eq. (12). As a result the gain margin becomes explicitly dependent on the synchronized state and hence the cross-coupling time delays.

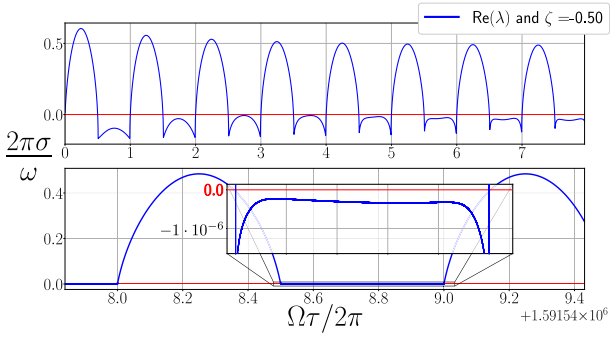

FIGURE 7. Perturbation response rate σ in a 2D square grid with 3 × 3 nearest neighbor mutually coupled PLLs as a function of the cross-coupling time delay. The delay margin is infinite and instabilities do not exist for this parameter configuration. PLL parameters are $\omega = 2\pi \cdot 1.0$ Hz, $K = 2\pi \cdot 0.185$ Hz/V, $\bar{\omega}^c = 2\pi \cdot 0.055$ Hz (first order RC), and $v = 1$.

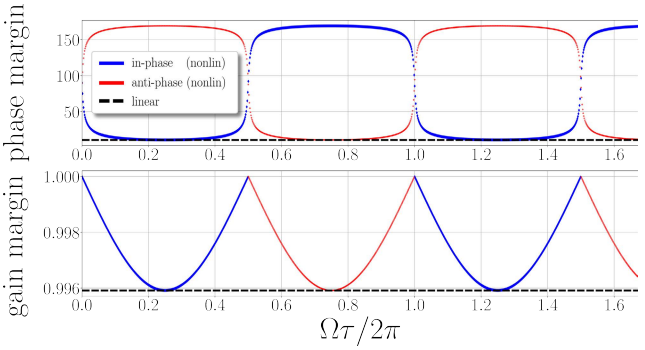

FIGURE 8. Phase and gain margin for a single PLL if in a network of $N = 2$ mutually cosinusoidal coupled PLLs as a function of the cross-coupling delay. The PLL parameters can be read off from Fig. 3. Note, that in- or anti-phase synchronization can only be stable for positive loop gain $\alpha > 0$.

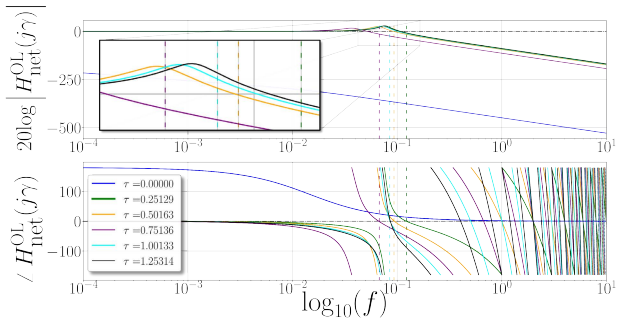

FIGURE 9. Bode plot for a network of $N = 2$ mutually cosinusoidal coupled PLLs using the network's open-loop transfer function, see numerator of Eq. (28). For $\tau > 0$ and after the first encirclement the subsequent phase crossover frequencies are periodic with half of the frequency associated to the time delay, i.e., $0.5\tau^{-1}$. PLL parameters can be read off from Fig. 10.

For the phase margin of PLL k with the pole at -1 we find

$$m_{\mathrm{p}}(\gamma_{\mathrm{c}}^{\mathrm{g}}) = \begin{cases} \pi - \arctan\left(\dfrac{\mathrm{Im}(H_k^{\mathrm{OL}}(i\gamma_{\mathrm{c}}^{\mathrm{g}}))}{\mathrm{Re}(H_k^{\mathrm{OL}}(i\gamma_{\mathrm{c}}^{\mathrm{g}}))}\right) & \text{if } \mathrm{Re}\left(H_k^{\mathrm{OL}}(i\gamma_{\mathrm{c}}^{\mathrm{g}})\right) > 0, \\ \arctan\left(\dfrac{\mathrm{Im}(H_k^{\mathrm{OL}}(i\gamma_{\mathrm{c}}^{\mathrm{g}}))}{\mathrm{Re}(H_k^{\mathrm{OL}}(i\gamma_{\mathrm{c}}^{\mathrm{g}}))}\right) & \text{if } \mathrm{Re}\left(H_k^{\mathrm{OL}}(i\gamma_{\mathrm{c}}^{\mathrm{g}})\right) < 0. \end{cases} \tag{19}$$

where $\gamma_{\mathrm{c}}^{\mathrm{g}}$ denotes the so-called gain crossover frequency. Note, that the critical frequencies $\gamma_{\mathrm{c}}^{\mathrm{g}}$ and $\gamma_{\mathrm{c}}^{\mathrm{p}}$ are also functions of the properties of the synchronized state and the cross-coupling time delays. The gain and phase margin of an individual PLL are periodic functions of the cross-coupling time delay. Their periods are equal to that of the synchronized state, see Fig. 8.

These concepts can also be defined for the transfer functions of networks of coupled PLLs and then be used to study the stability and properties of synchronized states, see III-B. In the following paragraph we will discuss this and introduce a definition of delay margin for networks of coupled PLLs. In the next section these results will then be showcased for the entrainment and mutual synchronization case for minimal example systems. We note here, that computing the determinant in Eq. (14) will always yield a term $(-1)^N$ since there is no self-coupling. Hence, the characteristic equation can be rearranged such that it represents an equivalent of an open-loop transfer function from which stability can be studied using phase- and gain margins. The poles would then be at one or minus one depending on whether N is odd or even.

1) DISCUSSION

For the operation of synchronization layers in applications the locking and characteristic perturbation response times are important measures. For $\sigma = 0$ the perturbation response frequencies $\gamma_{\mathrm{c}} \neq 0$ at the critical point can be calculated squaring and adding the real and imaginary part of Eq. (15) Ideally perturbations to a synchronized state decay fast. Such perturbation decay times can be approximated for stable synchronized states by $t^{\mathrm{r}} = |\sigma_0^{-1}|$ and are computed as

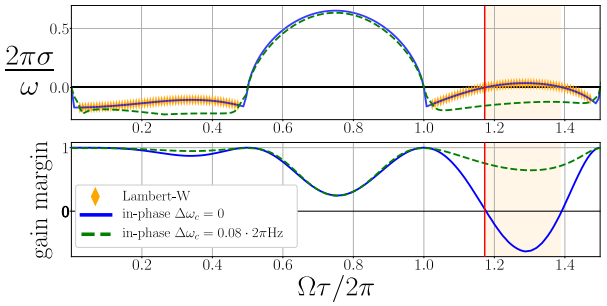

FIGURE 10. Perturbation response rate σ and gain margin for a network of $N = 2$ mutually coupled PLLs as a function of the cross-coupling time delay. Heterogeneity in the cut-off frequencies of the PLLs' LFs can stabilize the synchronized state. The PLL parameters are $\bar{\omega}^{\mathrm{c}} = 2\pi \cdot 0.055$ Hz (first order LF), $\omega = 2\pi \cdot 1.0$ Hz, $K = 2\pi \cdot 0.185$ Hz/V, and $\nu = 1$. Delay margin for the case of homogeneous cut-off frequencies is labeled by the red line.

discussed in Sec. III-B. In Figs. 5 and 6 it can be observed that the perturbation response rate alternates between positive and negative values as a function of the cross-coupling time delay. There is a critical time delay above which the perturbation response is underdamped, see Fig. 6. For such underdamped response the $|\sigma_0|$ of consecutive stable regimes tends to decrease. In the overdamped case however, the $|\sigma_0|$ of consecutive stable regimes increases with increasing time delay. Hence, there is a globally optimal perturbation decay for the value of the time delay where overdamped decay transitions to underdamped perturbation decay. Furthermore, within each stable regime there are values of the time delays for which perturbations decay optimally, see Fig. 6.

Considering that stable synchronized solutions can only exist for $\alpha > 0$, i.e., positive steady state loop gain, the question arises how α relates to the perturbation decay rate. It is a periodic function of the cross-coupling time delay, see Fig. 4. However, its magnitude is independent of the time delay and therefore cannot account for the nonlinear change of the perturbation response. Studying the characteristic Eq. (15) at the critical point (setting $\lambda_{\mathrm{c}} = j\gamma_{\mathrm{c}}$) reveals that instabilities of synchronized states set in as the gain margin becomes negative for the first time. This can only occur when the stability condition in Eq. (16) is not fulfilled. Following this line of thought we define the *delay margin* of a network of coupled PLLs. It is obtained by computing at which cross-coupling time delay the gain margin of the

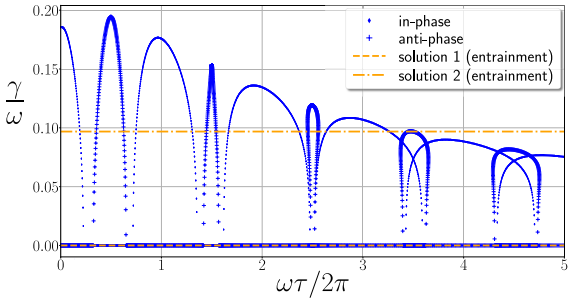

FIGURE 11. Frequency of perturbation response $\gamma = \mathrm{Im}(\lambda)$ vs the cross-coupling time delay τ in multiples of the intrinsic period of the PLL $T = 2\pi/\omega$. Rescaling γ with ω we express it in multiples of the intrinsic frequency. For system parameters see Fig. 3.

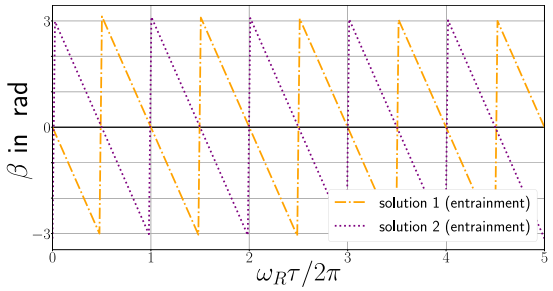

FIGURE 12. The phase difference $\beta \in [-\pi, \pi)$ of the PLL with respect to the phase of the reference that entrains is a linear function of the cross-coupling time delay. The PLLs parameters are $\omega_{\text{ref}} = 2\pi \cdot 1$ Hz, $\omega = 2\pi \cdot 1$ Hz, $K = 2\pi \cdot 0.02$ Hz/V, $\omega^{\text{c}} = 2\pi \cdot 1$ Hz, $v = 1$ and $h(x) = \sin(x)$.

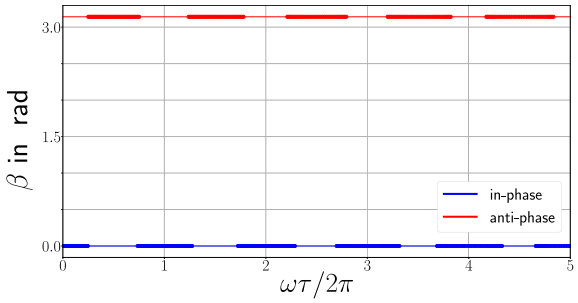

FIGURE 13. Phase difference $\beta \in [-\pi, \pi)$ between two mutually coupled PLLs as a function of the cross-coupling time delay. PLL parameters are $\omega = 2\pi \cdot 1$ Hz, $K = 2\pi \cdot 0.02$ Hz/V, $\omega^{\text{c}} = 2\pi \cdot 1$ Hz, $v = 1$ and $h(x) = \sin(x)$. Thick lines indicate where solutions are linearly stable.

network transfer function becomes negative for the first time, see Fig. 10. For identical PLLs and time delays an analytic expression for σ_0 in terms of the Lambert W-function can be obtained from Eq. (15)

$$\sigma_0 = -\frac{\omega^{\text{c}}}{2} + \frac{1}{\tau} W\left(-\frac{\omega^{\text{c}} \alpha\, \tau\, |\zeta_0|\, \sin(\gamma\tau - \Psi_0)}{2\gamma} e^{\frac{\omega^{\text{c}}\tau}{2}}\right), \quad (20)$$

with so far unknown γ.

$$\gamma_{\text{c}}^4 + \gamma_{\text{c}}^2 \left((\omega^{c})^2 - 2\alpha\omega^{\text{c}}\right) + \left(\alpha\omega^{\text{c}}\right)^2 \left(1 - |\zeta|^2\right) = 0. \quad (21)$$

Hence, frequencies γ_{c} for which the right hand side of Eq. (20) equals to zero represent the phase crossover frequencies at which the gain margin changes its sign. An example is shown in Fig. 10 where we plot the gain margin obtained from the network transfer function Eq. (28) in Sec. IV alongside with the approximation in Eq. (20) and the numerical solution for σ_0 of the full characteristic Eq. (27). Note that the stability analysis using the gain, phase and delay margin only reveals where synchronized states become unstable for the first time while $\alpha > 0$. It does not distinguish the stability of in- and anti-phase synchronized states. This information can be obtained solving the characteristic Eq. (14). The underdamped perturbation decay leads to shoulders in the power spectral density at frequencies $\Omega \pm \gamma$ that relate to the constant (underdamped) decay of noise induced perturbations to the synchronized state. γ denotes the frequency of the slowest perturbation response that is calculated solving Eq. (15), see Fig. 11. We want to remind the reader that the high frequency contributions of the PD output signal were assumed to be filtered ideally in the set of Eqs. (6). Therefore the instabilities that can be identified within the framework of these equations must relate to low frequency contributions in the PD signal to become amplified. This amplification leads to a periodic modulation of the control signal and consequently the VCO's instantaneous output frequency. Hence, if the gain margin changes its sign and becomes negative, e.g., see Fig. 9, spurious signals arise from the shoulders in the power spectrum. This can be observed in Fig. 9, where for time delay $\tau \geq 1.00133$ s the gain margin becomes negative at the phase crossover frequency. In the case of a network of 2 mutually delay-coupled PLLs this is defined by the phase crossing zero for the first time. Hence, we conclude that the architecture design process of network synchronization layers subject to considerable cross-coupling time delays requires, as shown in Sec. III, to take into account the state dependent properties of the network and its nodes.

IV. EXAMPLES OF NETWORK SYNCHRONIZATION

In this section we present two minimal example systems and discuss the main differences between entrainment and mutual synchronization. The differences are subtle and connected to the degrees of freedom in systems with these approaches to synchronization. Nonetheless they have far reaching consequences for network synchronization, systems design and applications. In summary it can be stated that without the exact knowledge of the cross-coupling time delays, in- and anti-phase synchronization can only be achieved using mutual synchronization, see Figs. 12 and 13. Since there is no reference frequency entrained into mutual synchronization layers, these can self-organize a common global frequency such that the phase-differences are zero. Therefore precise phase relations can be achieved without the necessity to know the exact values of all cross-coupling time delays. However, systems that synchronize mutually loose accuracy with respect to external reference oscillators or time-measures. In the last section we show time-series from simulations of synchronization dynamics in larger PLL networks and in the presence of dynamic noise.

A. ENTRAINMENT OF A PLL BY A REFERENCE SIGNAL

First, we revisit the case of an oscillator that is being entrained by a reference oscillator [50]. The reference oscillator has index R and receives no input from other oscillators in the network, i.e., all $c_{Rl} = 0$. For the phase difference β_{R1} between the reference and PLL 1 in an entrained state we find from the set of Eqs. (8) with $\Omega = \omega_{\text{ref}}$:

$$\beta_{R1} = -\omega_{\text{ref}} \tau_{R1}^{\text{e}} - v\, h^{-1}\left(\frac{\omega_{\text{ref}} - \omega_1}{K_1}\right) + v\, \phi^{\text{INV}}. \quad (22)$$

The terms independent of the time delay denote the actual instantaneous phase difference between the reference oscillator and the entrained PLL. These terms are related to

the detuning of the intrinsic frequencies $\Delta\omega = \omega_{\text{ref}} - \omega_1$ and the PLL's inverter state $\phi^{\text{INV}} \in \{0, \pi\}$. This instantaneous phase difference together with the time delay term $-\omega_{\text{ref}}\tau^{\text{e}}_{R1}$ represents the phase difference detected by the PLL at its phase-detector. Hence, the phase difference has a linear dependence on the effective coupling delay τ^{e}_{R1}, see Fig. 12. It can additionally be shifted due to oscillator heterogeneity $\Delta\omega$ rescaled by the divider. It can be observed that true in-phase synchronization can only be achieved for cross-coupling time delay values with a periodicity of the period of the reference frequency.

The perturbation dynamics can be read off from Eq. (10) and we find the closed-loop transfer function of the network

$$H^{\text{CL}}_{\text{net}}(\lambda) = e^{-\lambda\tau_{1R}}\left(1/H^{\text{FF}}(\lambda) + e^{-\lambda\tau^f_1}\right)^{-1}, \tag{23}$$

where the denominator denotes the characteristic Eq. (15) for $\zeta = 0$. Contrary to mutual synchronization, for entrainment the steady state loop gain becomes independent of the cross-coupling time delay. Analysis reveals the stable ($\sigma < 0$) and unstable ($\sigma \geq 0$) solution with phase differences $\{0, \pi\}$ for sinusoidal coupling, see Fig. 5. Note that for cosinusoidal and triangular coupling functions the solutions have phase differences $\{-\pi/2, \pi/2\}$.

B. TWO MUTUALLY DELAY-COUPLED PLLs

For two mutually coupled heterogeneous PLLs we find from the set of Eqs. (8) using $\beta_{21} = -\beta_{12}$

$$\begin{aligned}\Omega &= \omega_1 + K_1\, h\left(-\Omega\tau_{12} - \beta_{12}\right),\\ \Omega &= \omega_2 + K_2\, h\left(-\Omega\tau_{21} + \beta_{12}\right).\end{aligned} \tag{24}$$

Hence the phase differences of synchronized solutions are independent of the time delay if $\tau_{12} = \tau_{21}$, see Fig. 13, and

$$\beta_{12} = \frac{1}{2}\left(h^{-1}\left(\frac{\Omega-\omega_1}{K_1}\right) - h^{-1}\left(\frac{\Omega-\omega_2}{K_2}\right)\right). \tag{25}$$

Analyzing Eq. (25) for identical PLLs and time delays one finds two solutions for β equal to $\{0, \pi\}$ for sinusoidal and $\{-\pi/2, \pi/2\}$ for cosinusoidal-type coupling functions. Adding heterogeneity in the PLL parameters and time delays, the phase differences then deviate from these solutions [26].

From Eq. (10) the closed loop transfer functions of PLLs in a network of two heterogeneous mutually coupled PLLs can be found. Here we show the transfer function for PLL $k = 1$

$$\frac{q_1(\lambda)}{q_2(\lambda)} = H_1{}^{\text{CL}}(\lambda) = \frac{H^{\text{FF}}_{12}(\lambda)e^{-\lambda\tau_{12}}}{1 + e^{-\lambda\tau^f_1}H^{\text{FF}}_{12}(\lambda)}. \tag{26}$$

Given these expressions we identify the G_{kl} as $G_{12} = H_1{}^{\text{CL}}$ and $G_{21} = H_2{}^{\text{CL}}$, the closed-loop transfer functions of PLL 1 and 2. The characteristic equation for the network according to Eq. (14) is then given by

$$\det(\mathbf{G} - \mathbf{I}) = 1 - G_{12}G_{21} = 0\,. \tag{27}$$

Since this characteristic equation is the denominator of the closed-loop transfer function we can infer the equivalent to an open-loop network transfer function as $H^{\text{OL}}_{\text{net}}(\lambda) = H_1{}^{\text{CL}}(\lambda)H_2{}^{\text{CL}}(\lambda)$. From this we define the network's closed loop transfer function for a system of two mutually coupled heterogeneous PLLs

$$H^{\text{CL}}_{\text{net}}(\lambda) = \frac{H^{\text{OL}}_{\text{net}}(\lambda)}{1 - H^{\text{OL}}_{\text{net}}(\lambda)}\,. \tag{28}$$

Using this transfer function and the concept of gain and phase margin the stability of synchronized states can now be studied using Eqs. (17) and (19). Hence, it is not necessary to solve Eq. (14) numerically, see Fig. 10. The critical cross-coupling time delay that defines the delay margin is obtained by increasing the time delay until the gain margin calculated at the first phase crossover frequency becomes negative for the first time.

C. NETWORK SYNCHRONIZATION SIMULATIONS

According to the set of dynamic Eqs. (6) we simulate a system of $N = 64$ mutually coupled PLLs with noisy VCO output in the presence of cross-coupling time delays. The oscillators are arranged on a 2-dimensional square grid with nearest neighbor coupling and open boundary conditions. The simulation was carried out using the Euler method solving the set of Eqs. (6) for two sequential first order RC loop filters with a decoupling buffer. Its impulse response function in Laplace space is modeled by $\hat{p}(\lambda) = (1 + \tau^{\text{c}}\lambda/2)^{-2}$, where τ^{c} is the characteristic integration time of the two RC loop filters [17]. For every period T_ω of the free-running oscillators 55 samples were considered.

Using the theoretical tools presented in this work we adjusted the PLL parameters such that stable in-phase synchronization can be achieved for cross-coupling time delays that are equivalent to 39968 times the intrinsic periods of the PLLs, i.e., $\tau = 39968\,T_\omega$. For oscillators operating at

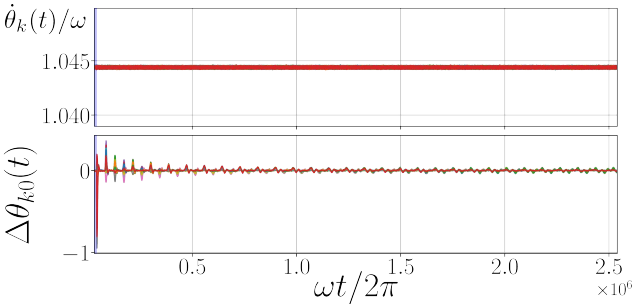

FIGURE 14. Frequency and phase differences as a function of time in a network of 8 × 8 nearest neighbor mutually coupled PLLs on a 2D square grid with open boundary conditions. The two cascaded passive and decoupled RC low pass filters are modeled by the Γ-distribution with shape parameter $\sigma = 2$ and integration time $\tau^{\text{c}} = (\omega^{\text{c}})^{-1} = 0.663$ ns. The PLL parameters are $\omega = 2\pi \cdot 24$ GHz, $K = 2\pi \cdot 1.2$ GHz/V, $\omega^{\text{c}} = 2\pi \cdot 2.4$ MHz, dynamic VCO Gaussian white noise variance $\sigma^{\text{VCO}} = 759$ kHz, cross-coupling time delay $\tau = 1.67\,\mu$s and division $\nu = 512$. The shaded regime denotes a part of the history. (upper plot) Instantaneous frequency of synchronized state $\dot{\phi}(t)$ normalized by the intrinsic DPLL frequency ω vs the time in multiples of the period of the free-running DPLL. (lower plot) Phase differences of all oscillators with respect to the oscillator with $k = 0$.

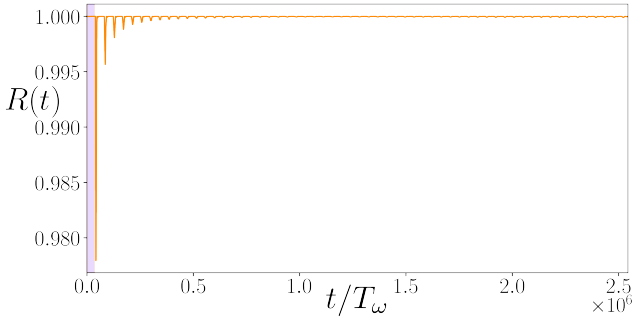

FIGURE 15. Kuramoto order parameter $R(t)$ vs time. It is defined as $R(t)\exp(i\Psi(t)) = 1/N\sum_k \exp(i\phi_k(t))$, i.e., $R(t) \to 1$ implies in-phase synchronization. For DPLL parameters see Fig. 14.

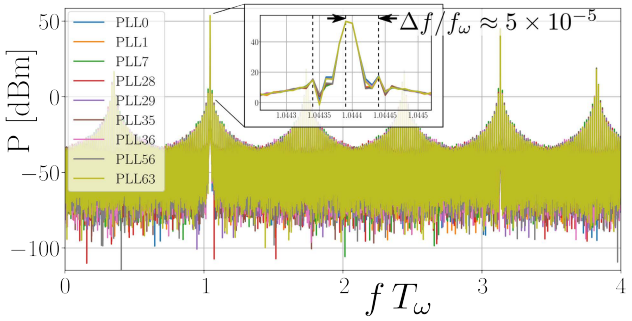

FIGURE 16. Power spectral densities for digital signals of the phases computed using the final $t = 4.2\,\mu$s of the time series and a boxcar window. The frequency resolution is $\Delta f \approx 240$ kHz, the sampling frequency $f_s = 1.32$ PHz. The oscillators at all corners and in the center of the grid with $k = \{0, 1, 7, 28, 29, 35, 36, 56, 63\}$ are shown. The inset is a zoom of the principal peak at $f = \Omega/2\pi$. DPLL parameters see Fig. 14.

24 GHz that equates to a time delay of $\tau = 1.67\,\mu$s and a distance of about 500 meters at signaling with the speed of light. To enable stable synchronization in such a system we choose the following PLL parameters: a divider with $\nu = 512$, a steady state loop gain of $\alpha = 1.49$ MHz/V, a Gaussian white noise with standard deviation $\sigma^{\text{VCO}} = 759$ kHz and LF cut-off frequency $f^c = 2.4$ MHz.

In Fig. 14 we show the transient dynamics of the frequencies and phase differences of all PLLs after switching on the cross-coupling. The Kuramoto order parameter $R(t)$ is plotted vs time in Fig. 15 and measures the phase coherence of the oscillators. It is defined as $R(t)\exp(i\Psi(t)) = 1/N\sum_k \exp(i\phi_k(t))$, where $\Psi(t)$ is the mean phase of all oscillators and $R(t)$ approaches 1 if all oscillators are in phase. A power spectral density (PSD) obtained for the oscillators at all corners and in the middle of the grid is shown in Fig. 16. An integer number of $p \approx 100000$ periods were analyzed to achieve a frequency resolution of $\Delta f \approx 240$kHz. The initial history is marked by the shaded regime from $t/T_\omega \in [0, \tau]$ in Fig. 14-15. During this initial history the oscillators are uncoupled and evolve with the frequency of the synchronized state such that they have a defined phase configuration when the coupling is switched on. The small frequency deviations and phase perturbations that are present when the coupling is activated lead to a transient response in the frequencies, order parameter and phase differences at the start of the simulation. Due to underdamped perturbation decay, Ω is weakly modulated during the transient period. This modulation becomes weaker over time, see time evolution of phase differences in Fig. 14. As can be seen from the time evolution of the phase differences in Fig. 15, neither the dynamic VCO noise, nor the perturbations cause phase slips to occur. The decaying initial perturbation can be observed at multiples of the cross-coupling time delays, as it echoes in the network. Since the time series used for computing the PSD is not free of perturbation response dynamics, these can be observed in form of the shoulders between the harmonics of the digital signal. As mentioned in Sec. III-C: underdamped perturbation responses lead to shoulders at $\Omega \pm \gamma$, where $\gamma/\omega = 3.48 \times 10^{-5}$ has been predicted by the numerical solution to the deterministic Eq. (15). This prediction is confirmed by the results of the time series simulation for which we find $\Delta f/f_\omega = 5 \times 10^{-5}$, see Fig. 16. Note that the small deviation may be caused by the perturbations and dynamic noise present in the time-series used to obtain the PSD.

V. SYSTEMS DESIGN FOR MUTUAL SYNCHRONIZATION

Here we address how the dynamics of mutual network synchronization can be guided to ensure robust operations as required by an application. The architecture design process for this synchronization solution requires the identification of the parameters that are fixed by the application and the utilization of the free parameters that can be used to control properties of self-organized synchronization. Introducing controllable elements in the PLL architecture and system design, frequency, phase relations and stability of self-organized synchronized states can be tuned, adjusted and optimized to different application scenarios. These controllable elements are however not required to make mutual synchronization work. However, such elements can help to optimize and adjust to changing requirements or environmental conditions. At the end of this section we discuss experimental results on mutual synchronization and current research activities related to the stability against large perturbations and noise in PLL networks.

A. TUNING THE GLOBAL FREQUENCY OF SYNCHRONIZED STATES

We have already pointed out the main difference between entrainment and mutual synchronization – for the latter the frequency of a synchronized state is not prescribed by a reference oscillator. Consequently, the global frequency that self-organizes for mutual synchronized states can drift when system parameters change due to, e.g., temperature variations or aging. Parameter drift induced changes of the global frequency can be limited by the maximum lock-in range of the PLLs and implementing control on, e.g., the intrinsic frequency to compensate such drifts via the tuning parameter V^{t}. Such compensation via the intrinsic PLL frequency can also

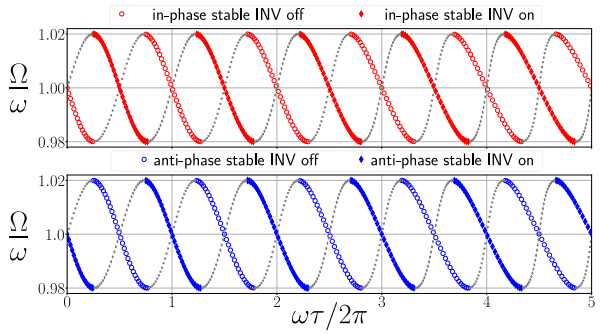

FIGURE 17. Frequency of synchronized state vs the time delay. Using the inverter in-phase synchronization can be achieved for all values of the time delay. PLL parameters are $K = 2\pi \cdot 0.02$ Hz/V, and $\omega^c = 2\pi \cdot 1.0$ Hz. For all other parameters see Fig. 3.

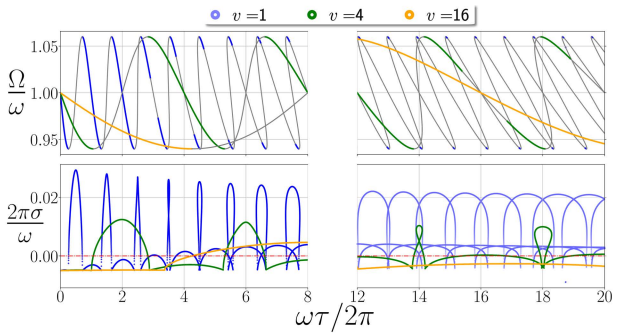

FIGURE 18. Frequency (first row) and linear stability (second row) as functions of the delay for different dividers. For system parameters see Fig. 3. The cut-off frequency of the first order LF changed to $\omega^c = 2\pi \cdot 0.25$ Hz.

be coupled to external frequency- and time references, which is subject to ongoing research.

B. THE ROLE OF AN INVERTER IN THE FEEDBACK PATH OF A PLL

For signals symmetric about half of their period, an active inverter in, e.g., the feedback introduces a frequency-independent phase-shift of π

$$\phi^{\text{INV}} = \begin{cases} \pi & \text{inverter active,} \\ 0 & \text{inverter inactive.} \end{cases} \tag{29}$$

Hence, for 2π-periodic coupling functions that implies that the sign of the coupling function changes, $h(x + \pi) = -h(x)$. This induces a sign change to the steady state loop gain α and the phase relations of, e.g., in- and anti-phase synchronized states shift by π. Hence, the inverter enables in- and anti-phase synchronized states for any value of the transmission-delay, where either one of these synchronized states exists and is stable. This can be used to achieve a specific synchronized state for any value of the cross-coupling delays, see Fig. 17.

C. FREQUENCY DIVIDER CHANGES DELAY INDUCED DYNAMICS

As is known, a frequency divider at the VCO output of each PLL in a PLL network effectively rescales the dynamics of synchronization processes. We find the following rescaling of the system parameters by the divisor v: for the effective time delay $\tilde{\tau}^e_{kl} = \tau^e_{kl}/v$, for the feedback time delay $\tilde{\tau}^f_k = \tau^f_k/v$, for the phase differences $\tilde{\beta}_{kl} = \beta_{kl}/v$, for the steady state loop gain $\tilde{\alpha}_{kl} = v\alpha_{kl}$, for the cut-off frequency of the LF's impulse response $\tilde{\omega}^c = 1/\tilde{\tau}^c = 1/(a_k\tilde{b}_k)$, and for the complex perturbation response rates $\tilde{\lambda} = \lambda v$. See Appendix VI for the derivations.

This scaling behavior has important consequences for the systems design of mutual network synchronization. It allows to achieve stable synchronization for cross-coupling time delays much larger than the time scale of the oscillations, see Fig. 18. As a consequence, the loop gain of the network decreases accordingly. The scaling of system parameters other than the time delay helps to understand how the PLL components can be designed to achieve optimal perturbation response dynamics. Note that the $\tilde{\beta}_{kl}$ are the phase differences between the cross-coupling signals and the β_{kl} are those between the high frequency output of the VCOs. Given that the system self-organizes its dynamics with respect to the cross-coupling signals at the divided VCO frequency, for in- and anti-phase synchronized states the phase differences β_{kl} will always be 0 for integer divider values v that are even, while being equal to $\beta_{kl} = \tilde{\beta}_{kl} = \{0, \pi\}$ for divider values v that are odd.

D. OPTIMAL PERTURBATION DECAY WITH HETEROGENEOUS COUPLING

It has been shown that tuning the coupling strengths in a PLL network to heterogeneous values can optimize the perturbation decay rates σ. Such heterogeneity can, e.g., be controlled via the gains in the feed forward path or the sensitivity of the VCOs. The achievable perturbation decay rates can be larger than that in the entrainment case where one clock entrains another by unidirectionally feeding into the PLL [26]. These decay rates are, in general, also larger than the perturbation decay rates in a system of mutually delay-coupled PLLs with identical gains in the feed-forward path.

E. SYNCHRONIZATION STABILIZATION WITH HETEROGENEOUS LF CUT-OFF FREQUENCIES

For PLL design the choice of the LF cut-off frequency is important. It affects the noise properties of the PLL and filters the higher order frequency components of the PD signal. However, it also introduces inertia to the systems dynamics and can destabilize mutual synchronized states. As shown in Fig. 10, the stability of these states can however be recovered by introducing heterogeneous LF cut-off frequencies while the mean cut-off frequency over the network remains constant [26]. Using this, mutual network synchronization may be optimized such that nodes which represent hubs in the network structure have especially low cut-off frequency for, e.g., optimal noise filtering and less strongly connected nodes compensate for these with larger cut-off frequencies.

F. INTERPLAY OF FILTERING, COUPLING AND FEEDBACK TIME SCALES

There are several important time scales associated to network synchronization systems, connected to the cross-coupling, feedback and filtering of signals. Whether these time scales dominate the dynamics depends on their mutual relation, as well as their relation to the time scale of the intrinsic oscillations of the PLLs. A tunable feedback time delay for example can be used for cross-coupling delay compensation. At the same time the perturbation decay rate usually decreases when increasing the feedback path time delay [26].

G. FREQUENCY SYNCHRONIZATION WITH TUNABLE PHASE DIFFERENCE

As discussed in the previous sections there are many different types of self-organized synchronized states that can emerge in networks of mutually coupled oscillators. We do not discuss synchronized states with time-dependent phase differences, such as e.g., spiraling waves solutions [29]. Whether in- or anti-phase, checkerboard or twist states with constant phase relations can exist depends on the system's setup. Using network topologies with open boundaries for example permits only in-phase and checkerboard synchronized states [39]. So called twist or splay states with specific constant phase relations between neighboring oscillators can exist in network topologies with periodic boundary conditions, e.g., ring or doughnut topology.

Moreover, the mutual phase differences between neighboring PLLs can be controlled by making the cross-coupling delays heterogeneous, while keeping the mean-delay in the system constant. With the mean cross-coupling time delays being constant, also the global frequency of a synchronized state is not affected when tuning the individual time delays. The phase differences however change as a linear function of the difference of the delays from the mean-delay [26].

H. EXPERIMENTS ON MUTUAL SYNCHRONIZATION

Some aspects discussed in this work have already been addressed in experiments. The effects of heterogeneity, specifically how phase relations can be tuned introducing delay-differences in a bidirectional coupling, and the stabilization of synchronized states when tuning cut-off frequencies to heterogeneous values have been shown experimentally in [26]. How network topology affects which synchronized states can exist has been addressed in [39]. Mutual synchronization and entrainment in the presence of cross-coupling time delay at microwave frequencies has been addressed in [2], [43]–[45], [50]. Questions related to phase noise and the stability of synchronized states against large perturbations have been addressed or are subject to ongoing research [59].

VI. DISCUSSION AND CONCLUSION

Precise phase synchronization can enable new applications in existing and next generation spatially distributed networks, such as sensor arrays, indoor navigation beacons, mobile communications infrastructure, the Internet of Things and autonomous mobility [60]–[64]. Localization with centimeter precision via time difference of arrival methods, for example, crucially depends on a network of precisely synchronized clocks with high time resolution [65]. The aforementioned systems often do not require to be accurate with respect to an absolute time reference, but instead their performance relies on the precise synchronization of the oscillators' phases within the network [66], [67]. In hierarchical synchronization approaches precise phase synchronization is difficult to achieve due to unavoidable cross-coupling time delays. In principle, the phase differences that arise in hierarchical synchronization could be compensated using delay compensation techniques. However, measuring the cross-coupling time delays requires an established, precise time-reference network. The time resolution of this established reference then limits how precisely the phase differences induced by the cross-coupling time delay can be inferred. In contrast, the concept of mutual network synchronization is a promising concept to fulfill the precision requirement. On its basis, spatially distributed time reference systems can be established since even considerable network cross-coupling time delays do not introduce phase differences. Once synchronized states have emerged over such networks, the oscillators' phases do not drift with respect to each other and perturbations to the phases and global frequency decay. Moreover, the precision of mutual synchronization in the presence of noise has been shown to scale advantageously with network size [6]. If necessary, a connection to absolute time references can be established. However, Lindsey *et al.* [6] also stated, that mutual synchronization has the disadvantage of the ''*complexity of its implementation*''. It is owed to the difficult mathematical analysis of the model in its most general form. This work addresses precisely this challenge, the complexity of the implementation of mutual network synchronization. It shows how stable synchronized states can be achieved in the presence of large cross-coupling time delays and for arbitrary network topology and loop filters. Analyzing a mathematical model for mutually delay-coupled phase oscillators with inert response characteristics, the guidance of self-organized synchronization dynamics towards robust synchronized states with specific properties is discussed.

This work presents a theoretical framework within which network synchronization can be studied and analyzed in large networks, and in the presence of significant cross-coupling time delays. Previous work, see e.g. [6], [51], linearized the nonlinear interactions related to the coupling. As a result, the PLL's steady state loop gain, and phase and gain margins were only determined by the properties of the PLL nodes, such as the transfer functions and constant component gains. Our analysis takes into account the nonlinear coupling terms and predicts different asymptotic dynamics for networks of mutually delay-coupled oscillators, see e.g., Fig. 3 for the comparison to previous work. As shown in Fig. 4, accounting for the nonlinear coupling also reveals that the loop gain of a PLL is not fixed but depends on the synchronized state

that emerges in the network. This allowed us to extend the definition of the steady state loop gain, and the phase and gain margins. Furthermore, we derived the network's open-loop transfer function from which a network gain margin can be calculated. The generalized network gain margin depends explicitly on the cross-coupling time delay and can be used to define a delay margin. This delay margin denotes the smallest time delay for which the gain margin of the network becomes negative, and the synchronized state unstable, see Fig. 10. Note, that this does not rule out stable synchronization for larger time delays. Moreover, when accounting for the nonlinear interaction terms, phenomena like the multistability of synchronized states and the properties of such states can be predicted and studied. These properties include the frequency of the oscillators in the synchronized state, their phase relations and the perturbation response rates of the perturbation modes. Hence, applying the theoretical tools introduced here, the stability and robustness of synchronized states with respect to weak perturbations can be predicted using Eq. (14), see results in e.g., Fig. 7-10. For large networks this can require to solve the characteristic equations numerically. In order to identify fast and efficiently the parameter regimes suitable for operating a large network of oscillators synchronously, we provide a stability condition in Eq. (16). It is sufficient to predict the stability of synchronized states. This condition generalizes a condition provided in [6] and now includes the state dependent steady-state loop gain, and the network topology. Compared to the result presented in [55], it also takes into account the network topology. Analyzing the stability condition also reveals that frequency synchronization is possible for any value of the cross-coupling time delay, see Fig. 7. Thereby, we address the complexity of implementing mutual synchronization in technical application, e.g., in smart grids, ad-hoc network structures, sensor arrays, radar applications and distributed/cell-free massive MIMO. Furthermore, we present examples of minimal networks that show how the theoretical tools can be applied and compare entrainment to mutual synchronization. In numerical simulations we show synchronization in networks of $N = 64$ mutually coupled PLLs in the presence of large time delays and oscillator noise.

The predictive power of our results also provides the means to optimize synchronization dynamics in mutual network synchronization. It can, for example, improve with component heterogeneity, see Fig. 10. There, it is shown how tuning the cut-off frequencies of the loop filters in a system of two mutually coupled phase-locked loops to heterogeneous values can stabilize a synchronized state. Furthermore, the prediction of the perturbation response rates using Eq. (14) allows to quantify the robustness of synchronized states with respect to small perturbations. It enables the optimization of the time scales with which perturbations decay.

When implementing mutual network synchronization in an application, the predictions of the nonlinear model can be used to guide the design of the synchronization layer. The following steps need to be taken. First, the requirements set by the application need to be identified, e.g., the frequency at which a system operates, the phase differences that are allowed, the time scales associated to the perturbation response, and the spectral properties of the output signals. In a second step the parameters that are fixed by the properties of the synchronization layer need to be identified, such as the minimum cross-coupling time delays between coupled nodes and the loop filter cut-off frequency. Given the fixed parameters, the theoretical framework introduced here can then be used to calculate how the free parameters of the PLLs and the network need to be adjusted to achieve stable synchronization for phase-locked synchronized states, see Sec. V. Note for example, that the condition in Eq. (16) implies a limit on the PLLs loop gain, and hence on its ability to react to perturbations. This is relevant since the cut-off frequency of the loop filter is usually fixed by the requirement to sufficiently damp the high frequency components of the phase detector.

Previous research suggests, that synchronization can be achieved robustly in the presence of noise and heterogeneity [26], [68]. However, further research into the effects of noise on the dynamics of synchronization is necessary to quantify the quality of synchronized states.

APPENDIX A
NONLINEAR VOLTAGE CONTROLLED OSCILLATORS

In general, the instantaneous frequency of a voltage controlled oscillator (VCO) as a function of the control signal can be written as

$$\dot{\phi}_k(t) = y\left(x_k^{\mathrm{c}}(t)\right), \tag{30}$$

where $y(\cdot)$ denotes the functional form of the VCO response. It depends on the architecture of the VCO and is usually a nonlinear function of the input voltage. For small changes of the control signal we can linearize the function around the operating point $x_k^{\mathrm{c,op}}$. The linearized function then has the form

$$\dot{\phi}_k(t) = y\left(x_k^{\mathrm{c,op}}\right) + y'\left(x_k^{\mathrm{c,op}}\right)\left(x_k^{\mathrm{c}}(t) - x_k^{\mathrm{c,op}}\right), \tag{31}$$

where $y(x_k^{\mathrm{c,op}})$ relates to the intrinsic frequency of the VCO set by, e.g., the tuning voltage V^{t}, and $y'(x_k^{\mathrm{c,op}})$ denotes the slope of the VCO's response at the operating point. For nonlinear VCO response we find using Eq. (30) and the set of Eqs. (1)-(2)

$$\dot{\phi}_k(t) = y\left(V^{\mathrm{s}} + G_k \sum_{l=1}^{N} \tilde{c}_{kl} \int_0^{\infty} \mathrm{d}u\, p_k(u) h\left(\frac{\delta\phi_{kl}(u,\tau)}{v} + \phi_k^{\mathrm{INV}}\right)\right), \tag{32}$$

where $V^{\mathrm{s}} = V^{\mathrm{t}} + G^{\mathrm{PD}} V^{\mathrm{b}}$ denotes the sum of bias and tuning voltage, $\tilde{c}_{kl} = c_{kl}/n(k)$, and G_k denotes the product of the

feed-forward path gains of PLL k. All other quantities are defined in the main text. We then analyze synchronized solutions making the ansatz $\theta_k(t) = \Omega t + \beta_k + \epsilon\, q_k(t)$. Expanding about the synchronized state for small perturbations ($\epsilon \ll 1$) we find that the properties of the synchronized state can be calculated via a set of N coupled equations

$$\Omega = y\left(V^{\mathrm{s}} + G_k \sum_{l=1}^{N} \tilde{c}_{kl}\, h\left(\frac{-\Omega\tau - \beta_{kl}}{v} + \phi_k^{\mathrm{INV}}\right)\right). \quad (33)$$

For the dynamics of the perturbations we obtain

$$\dot{q}_k(t) = \sum_{l=1}^{N} \tilde{c}_{kl}\alpha_{kl}^{*} \int_0^{\infty} \mathrm{d}u\, p_k(u)\left(q_l(t-u-\tau) - q_k(t-u-\tau^f)\right), \quad (34)$$

where $\alpha_{kl}^{*} = \frac{G_k}{v} y'\left(V^{\mathrm{s}} + \Xi\right) h'\left((-\Omega\tau - \beta_{kl})/v + \phi_k^{\mathrm{INV}}\right)$ and $\Xi = G_k \sum_{l=1}^{N} \tilde{c}_{kl}\, h\left((-\Omega\tau - \beta_{kl})/v + \phi_k^{\mathrm{INV}}\right)$. The constant sensitivity K^{VCO} has now been replaced by a nonlinear (induced by the architecture design) and state-dependent (depends on the properties of the synchronized state) sensitivity. Hence, α^{*} is the steady state loop gain for a nonlinear VCO response.

APPENDIX B
INTERNAL DYNAMICS OF DIGITAL PHASE-LOCKED LOOPS

From Eq. (5) in Sec. II-B we find for XOR phase-detector elements with no external input and digital feedback signals

$$\dot{\phi}(t) = \omega_0 + K^{\mathrm{VCO}} \int_0^{\infty} \mathrm{d}u\, p(u)\left(V^{\mathrm{t}} + x^{\mathrm{PD}}\left(\phi(t-u-\tau^f)\right)\right), \quad (35)$$

where G^{PD} denotes the gain of the phase-detector (PD), and $x^{\mathrm{PD}}(t) = G^{\mathrm{PD}}\, 0.5 \cdot (V^{\mathrm{b}} + \Pi(\phi))$ denotes a digital PD output signal. V^{b} denotes the biasing voltage and $\Pi(\phi)$ is a square wave function with constant peak-to-peak amplitude $2A$ and Fourier representation

$$\Pi(\phi) = \frac{4A}{\pi} \sum_{i=0}^{\infty} \frac{\sin\left([2i+1]\,\phi\right)}{2i+1}. \quad (36)$$

Hence, the PD output signal $x^{\mathrm{PD}}(t)$ can, e.g., be centered about zero voltage for $V^{\mathrm{b}} = 0$ or tuned to be a digital signal with binary voltage output states $\{0,\ A\}$ for $V^{\mathrm{b}} = A$.

We set out to find the intrinsic frequency of the PLL as a function of the intrinsic VCO frequency and the properties of the loop filter (LF) represented by $p(u)$, specifically its cut-off frequency ω^{c}. The free-running PLL with a constant intrinsic frequency ω implies for the phase $\phi(t) = \omega t + \beta$, where β denotes an arbitrary initial phase. Using this in Eq. (35) while setting $V^{\mathrm{t}} = 0$ as it only adds a constant tuning voltage we find

$$\omega = \omega_0 + \frac{K^{\mathrm{VCO}} G^{\mathrm{PD}}}{2} \times \int_0^{\infty} \mathrm{d}u\, p(u)\left(V^{\mathrm{b}} + \Pi\left(\omega(t-u-\tau^f) + \beta\right)\right). \quad (37)$$

Hence, a constant intrinsic PLL frequency in the free-running PLL case is only possible if the LF ideally filters all frequency contributions on the r.h.s. of Eq. (37) such that it becomes constant. From Eq. (36) we find that the lowest order frequency contribution is proportional to $\mathcal{O}(\omega_0)$, the intrinsic frequency of the VCO and therefore impose $\omega^{\mathrm{c}} \ll \omega_0$. Hence, for ideally filtered high frequency contributions of the PD signal, the intrinsic frequency of a free-running digital PLL is given by

$$\omega = \omega_0 + \frac{K^{\mathrm{VCO}} G^{\mathrm{PD}} V^{\mathrm{b}}}{2}. \quad (38)$$

Note that for mutual synchronization applications it can be advantageous to design PD circuitry with tunable gain G^{PD}. To prevent the intrinsic PLL frequency being dependent on the gains the operational point of the PD elements can be shifted to zero using $V^{\mathrm{b}} = 0$.

APPENDIX C
RESCALING OF TIME DELAYS USING THE DIVIDER

Division of the feedback and cross-coupling signals in a network of coupled PLLs changes the properties and stability of synchronized states. Introducing time delays and phase differences $\tilde{\tau}_{kl}^{\mathrm{e}} = \tau_{kl}^{\mathrm{e}}/v$ and $\tilde{\beta}_{kl} = \beta_{kl}/v$ rescaled by the divisor, the set of Eqs. (8) for properties of a synchronized state read

$$\Omega = \omega_k + \frac{K_k}{n(k)} \sum_{l=1}^{N} c_{kl}\, h\left(-\Omega\tilde{\tau}_{kl}^{\mathrm{e}} - \tilde{\beta}_{kl} + \phi_k^{\mathrm{INV}}\right). \quad (39)$$

Hence, the frequencies of synchronized states Ω depend on the rescaled time delay $\tilde{\tau}_{kl}^{\mathrm{e}}$. This amounts essentially to stretching or compressing along the delay-dimension. The phase differences $\tilde{\beta}_{kl}$ denote differences with respect to the signals with divided frequency. The system self-organizes with respect to the cross-coupling signals and its properties $\tilde{\Omega} = \Omega/v$ and $\tilde{\beta}_{kl}$.

The stability of synchronized states is affected as follows. We express the steady state loop gains for each individual external input path l of PLL k in terms of the rescaled time delays and phase differences which yields

$$\tilde{\alpha}_{kl} = v\alpha_{kl} = K_k\, h'\left(-\Omega\tilde{\tau}_{kl}^{\mathrm{e}} - \tilde{\beta}_{kl} + \phi_k^{\mathrm{INV}}\right). \quad (40)$$

Furthermore we can define $\tilde{\lambda} = \lambda v$ and $\tilde{\tau}_k^f = \tau_k^f/v$ with which we can rewrite the set of Eqs. (13)

$$G_{kl} = \frac{c_{kl}}{n(k)}\, \tilde{\alpha}_{kl} e^{-\tilde{\lambda}\tilde{\tau}_{kl}^{\mathrm{e}}} \times \left(\frac{\tilde{\lambda}}{\hat{p}_k\left(\tilde{\lambda};\, a_k,\, \tilde{b}_k\right) e^{-\tilde{\lambda}\tilde{\tau}_k^f}} + \sum_{l'=1}^{N} \frac{c_{kl'}}{n(k)} \tilde{\alpha}_{kl'}\right)^{-1}. \quad (41)$$

This amounts to a rescaling of the scale parameter $\tilde{b}_k = b_k/v$ of the Γ-distribution and hence effectively the integration time and cut-off frequency $\tilde{\omega}_k^c = 1/\tilde{\tau}_k^c = 1/(a_k\tilde{b}_k)$ of the LF.

APPENDIX D
STABILITY ANALYSIS IN DYNAMICAL SYSTEMS THEORY

From the set of Eqs. (6) for $\tau_{kl}^f = \tau_k^f$ and using the ansatz Eq. (7) we obtain from $\mathcal{O}(\epsilon^1)$ the perturbation dynamics

$$\dot{q}_k(t) = \sum_{l=0}^{N} \frac{c_{kl}\alpha_{kl}}{n(k)} \int_0^\infty \mathrm{d}u\, p(u) \times \Big(q_l(t-u-\tau_{kl}) - q_k(t-u-\tau_k^f) \Big). \quad (42)$$

This expression is obtained from inserting the ansatz Eq. (7) into the set of Eqs. (6) and then expanding the coupling function $h(\cdot)$ to first order with respect to its argument. Hence, the properties of the synchronized state whose stability is studied are absorbed into the feed-forward path loop gain α_{kl}. Introducing $\tilde{c}_{kl} = c_{kl}/n(k)$ and Laplace transformation yields

$$q_k(\lambda) = \frac{\sum_{l=1}^N \tilde{c}_{kl}\,\alpha_{kl} e^{-\lambda(\tau_{kl}-\tau_k^f)}}{\left(\frac{\lambda}{\hat{p}_k(\lambda)e^{-\lambda\tau_k^f}} + \sum_{l'=1}^N \tilde{c}_{kl'} a_{kl'} \right)} q_l(\lambda). \quad (43)$$

Hence, there is no straightforward way to define a transfer function by rearrangement to $H^{\mathrm{OL}}(\lambda) = q_k(t)/\sum_l q_l(t)$. The properties of the PLL nodes and the network are intricately coupled. Hence, a closed-loop transfer function of a PLL with more than one input can only be defined if all PLLs and cross-coupling time delays in the network are identical. In a matrix form we can write $\zeta \cdot \mathbf{q} = \mathbf{G} \cdot \mathbf{q}$, where $\zeta = 1$, and $\mathbf{q} = (q_1, q_2, \ldots, q_N)$ is the vector of perturbations. The matrix elements of $\mathbf{G}$ then are

$$G_{kl} = \frac{c_{kl}}{n(k)}\, a_{kl} e^{-\lambda(\tau_{kl}-\tau_k^f)} \left(\frac{\lambda}{\hat{p}_k(\lambda)e^{-\lambda\tau_k^f}} + \sum_{l'=1}^{N} \frac{c_{kl'}}{n(k)} a_{kl'} \right)^{-1}. \quad (44)$$

Hence, the characteristic equation can then be obtained from $\det(\mathbf{G}-\mathbf{I}) = 0$. Note that we assume each PLL has a *coupling capacity* which is equally distributed towards its $n(k)$ inputs. As consequence the sum over each row of the matrix $\tilde{\mathbf{C}} = (\tilde{\mathbf{c}}_{\mathbf{kl}})$ equals to one, or in terms of $\mathbf{C}$ to the $n(k)$ external inputs.

We define the contribution q_{kl} to the phase perturbation of input path l to PLL node k as

$$q_{kl}(\lambda) = \alpha_{kl} \frac{\hat{p}_k(\lambda)}{\lambda} q_l(\lambda), \quad (45)$$

where α_{kl} defines the steady state loop gain of each individual path l and depends on the time delays and the component heterogeneity, specifically in the case of mutually coupled PLLs. Hence, we define Eq. (11) from Eq. (45) using $H_{kl}^{\mathrm{FF}} = q_{kl}/q_k$. The relation between all inputs $q_l(\lambda)$ and the output $q_k(\lambda)$ of the circuitry is

$$q_k(\lambda) = \sum_{l=1}^{N} \tilde{c}_{kl} q_{kl}(\lambda) = \sum_{l=1}^{N} \tilde{c}_{kl}\alpha_{kl} \frac{\hat{p}_k(\lambda)}{\lambda} q_l(\lambda), \quad (46)$$

where the sum represents the adder component that adds the different external inputs. $\sum_{l=1}^N \tilde{c}_{kl}\alpha_{kl}$ denotes the mean steady state loop gain of PLL k with respect to all external inputs l. Note that the steady-state loop gain is a periodic function of the time delay τ. For analog PDs, i.e., multipliers it does not matter whether this addition happens before or after the PD. For digital signals and XOR PDs the addition has to be performed after the PDs. Analyzing Eq. (10) we notice, that the stability of a PLL node depends on the properties of all feed-forward paths $H_{kl}^{\mathrm{FF}}(\lambda)$ of PLL k. As a consequence, the stability of a PLL network, given by analyzing the determinant of the matrix $\mathbf{G}$, depends on the properties of all PLL's feed-forward paths $H_{kl}^{\mathrm{FF}}(\lambda)$. Using Eq. (11) we can identify

$$G_{kl} = \left(\tilde{c}_{kl} \frac{H_{kl}^{\mathrm{FF}}(\lambda)\, e^{-\lambda(\tau_{kl}-\tau_k^f)}}{1+e^{-\lambda\tau_k^f} \sum_{l'=1}^N \tilde{c}_{kl'} H_{kl'}^{\mathrm{FF}}(\lambda)} \right), \quad (47)$$

and thereby establish a connection between H_{kl}^{FF} and G_{kl}.

For identical cross-coupling delays and PLL parameters the properties of PLLs decouple from those of the network topology in Eq. (43). Hence, $\alpha_{kl} = \alpha$, $H_{kl}^{\mathrm{FF}}(\lambda) = H^{\mathrm{FF}}(\lambda)$ and Eq. (43) can be written

$$q_k(\lambda) = H_{\mathrm{PLL}}^{\mathrm{CL}}(\lambda) \sum_{l=1}^{N} \tilde{c}_{kl} q_l(\lambda). \quad (48)$$

The closed loop transfer function $H_{\mathrm{PLL}}^{\mathrm{CL}}(\lambda)$ can now be defined

$$H_{\mathrm{PLL}}^{\mathrm{CL}}(\lambda) = \frac{H^{\mathrm{FF}}(\lambda) e^{-\lambda(\tau-\tau^f)}}{\left(1 + e^{-\lambda\tau^f} H^{\mathrm{FF}}(\lambda) \sum_{l'=1}^N \tilde{c}_{kl'}\right)}. \quad (49)$$

Hence, $\mathbf{G} = \mathbf{H}_{\mathrm{PLL}}^{\mathrm{CL}}(\lambda) \cdot \tilde{\mathbf{C}}$ and Eq. (14) simplifies to $H_{\mathrm{PLL}}^{\mathrm{CL}}(\lambda)^{-1}\, \mathbf{q} = \tilde{\mathbf{C}} \cdot \mathbf{q}$ which leads to the characteristic Eq. (15).

ACKNOWLEDGMENT

The authors would like to thank D. Schmidt, D. Jörg, A. Pollakis, J. Wagner, M. Thayyil, G. Fettweis, and G. Ascheid for inspiring discussions and also would like to thank the cooperation of the Centre for Tactile Internet With Human-in-the-Loop (CeTi), a Cluster of Excellence at TU Dresden, in the area of millimeter-wave circuits. The work on this topic was initiated within the Cluster of Excellence Center for Advancing Electronics Dresden. *(Lucas Wetzel and Dimitrios Prousalis contributed equally to this work.)*

REFERENCES

[1] A. C. Oates, L. G. Morelli, and S. Ares, "Patterning embryos with oscillations: Structure, function and dynamics of the vertebrate segmentation clock," *Development*, vol. 139, no. 4, pp. 625–639, Feb. 2012.

[2] E. Koskin, D. Galayko, and E. Blokhina, "A concept of synchronous ADPLL networks in application to small-scale antenna arrays," *IEEE Access*, vol. 6, pp. 18723–18730, 2018.

[3] A. Solovev and B. M. Friedrich, "Synchronization in cilia carpets: Multiple metachronal waves are stable, but one wave dominates," *New J. Phys.*, vol. 24, no. 1, Jan. 2022, Art. no. 013015.
[4] V. Flunkert, S. Yanchuk, T. Dahms, and E. Schöll, "Synchronizing distant nodes: A universal classification of networks," *Phys. Rev. Lett.*, vol. 105, Dec. 2010, Art. no. 254101.
[5] A. Pikovsky, M. G. Rosenblum, and J. Kurths, *Synchronization, A Universal Concept in Nonlinear Sciences*. Cambridge, U.K.: Cambridge Univ. Press, 2001.
[6] W. Lindsey, F. Ghazvinian, W. C. Hagmann, and K. Dessouky, "Network synchronization," *Proc. IEEE*, vol. 73, no. 10, pp. 1445–1467, Oct. 1985.
[7] A. Gersho and B. J. Karafin, "Mutual synchronization of geographically separated oscillators," *Bell Syst. Tech. J.*, vol. 45, no. 10, pp. 1689–1704, Dec. 1966.
[8] M. B. Brilliant, "The determination of frequency in systems of mutually synchronized oscillators," *Bell Syst. Tech. J.*, vol. 45, no. 10, pp. 1737–1748, Dec. 1966.
[9] M. Karnaugh, "A model for the organic synchronization of communications systems," *Bell Syst. Tech. J.*, vol. 45, no. 10, pp. 1705–1735, Dec. 1966.
[10] R. D. Cideciyan, "Network synchronization techniques in the presence of oscillator drift and time-varying delay," ProQuest dissertation, Univ. Southern California Digit. Library (USC.DL), 2015. [Online]. Available: https://uosc.primo.exlibrisgroup.com/discovery/fulldisplay?docid=cdi_proquest_journals_1642793631&context=PC&vid=01USC_INST:01USC&lang=en&search_scope=MyInst_and_CI&adaptor=Primo%20Central&tab=Everything&query=any,contains,Network%20synchronization%20techniques%20in%20the%20presence%20of%20oscillator%20drift%20and%20time-varying%20delay, doi: 10.25549/USCTHESES-C30-503129.
[11] K. G. Shin and P. Ramanathan, "Transmission delays in hardware clock synchronization," *IEEE Trans. Comput.*, vol. C-37, no. 11, pp. 1465–1467, Nov. 1988.
[12] J. J. M. Wang, "On delay, Doppler and clock instabilities compensation techniques in synchronization networks," ProQuest dissertation, 1986. [Online]. Available: https://uosc.primo.exlibrisgroup.com/discovery/fulldisplay?docid=cdi_proquest_journals_1643213468&context=PC&vid=01USC_INST:01USC&lang=en&search_scope=MyInst_and_CI&adaptor=Primo%20Central&tab=Everything&mode=Basic
[13] E. Brewer, "Spanner, TrueTime and the CAP theorem," Google, Tech. Rep., 2017. [Online]. Available: https://research.google/pubs/pub45855/
[14] M. Zimmerling, L. Mottola, and S. Santini, "Synchronous transmissions in low-power wireless: A survey of communication protocols and network services," *ACM Comput. Surv.*, vol. 53, no. 6, pp. 1–39, Nov. 2020.
[15] L. Wetzel, F. Jülicher, D. Jörg, G. Fettweis, W. Rave, and A. Pollakis, "Self-synchronizable network," European Patent 2 957 982, Jun. 2014. [Online]. Available: https://patents.google.com/patent/EP2957982B1/tr
[16] K. P. O'Keeffe, H. Hong, and S. H. Strogatz, "Oscillators that sync and swarm," *Nature Commun.*, vol. 8, no. 1, p. 1504, 2017.
[17] R. C. Mancini, *Op Amps for Everyone: Design Reference*, 2nd ed. London, U.K.: Newnes, 2003. [Online]. Available: https://cds.cern.ch/record/645193
[18] P. Tosato, D. Facinelli, M. Prada, L. Gemma, M. Rossi, and D. Brunelli, "An autonomous swarm of drones for industrial gas sensing applications," in *Proc. IEEE 20th Int. Symp. World Wireless, Mobile Multimedia Netw. (WoWMoM)*, Jun. 2019, pp. 1–6.
[19] M. S. Innocente and P. Grasso, "Self-organising swarms of firefighting drones: Harnessing the power of collective intelligence in decentralised multi-robot systems," *J. Comput. Sci.*, vol. 34, pp. 80–101, May 2019.
[20] O. Shrit, S. Martin, K. Alagha, and G. Pujolle, "A new approach to realize drone swarm using ad-hoc network," in *Proc. 16th Annu. Medit. Ad Hoc Netw. Workshop (Med-Hoc-Net)*, Jun. 2017, pp. 1–5.
[21] V. E. Beneš, "Unpublished work," Tech. Rep., 1959.
[22] J. P. Runyon, "Reciprocal timing of time division switching centers," U.S. Patent 3 050 586, Aug. 21, 1962.
[23] A. J. Goldstein, "Unpublished work," Tech. Rep., 1963.
[24] A. Pollakis, L. Wetzel, D. J. Jörg, W. Rave, G. Fettweis, and F. Jülicher, "Synchronization in networks of mutually delay-coupled phase-locked loops," *New J. Phys.*, vol. 16, no. 11, Nov. 2014, Art. no. 113009.
[25] D. J. Jörg, A. Pollakis, L. Wetzel, M. Dropp, W. Rave, F. Jülicher, and G. Fettweis, "Synchronization of mutually coupled digital PLLs in massive MIMO systems," in *Proc. IEEE Int. Conf. Commun. (ICC)*, Jun. 2015, pp. 1716–1721.
[26] N. Punetha and L. Wetzel, "How clock heterogeneity affects synchronization and can enhance stability," 2019, *arXiv:1908.11085*.
[27] J. Hale and S. V. Lunel, *Introduction to Functional Differential Equations*. New York, NY, USA: Springer-Verlag, 1993.
[28] S. M. L. O. Diekmann, A. S. van Gils, and H.-O. Walther, *Delay Equations, Functional-, Complex-, and Nonlinear Analysis*. New York, NY, USA: Springer-Verlag, 1993.
[29] M. K. S. Yeung and S. H. Strogatz, "Time delay in the Kuramoto model of coupled oscillators," *Phys. Rev. Lett.*, vol. 82, no. 3, pp. 648–651, Jan. 1999.
[30] F. Mazenc, S. Mondie, and S. I. Niculescu, "Global asymptotic stabilization for chains of integrators with a delay in the input," *IEEE Trans. Autom. Control*, vol. 48, no. 1, pp. 57–63, Jan. 2003.
[31] J.-P. Richard, "Time-delay systems: An overview of some recent advances and open problems," *Automatica*, vol. 39, no. 10, pp. 1667–1694, 2003.
[32] V. L. Kharitonov, S.-I. Niculescu, J. Moreno, and W. Michiels, "Static output feedback stabilization: Necessary conditions for multiple delay controllers," *IEEE Trans. Autom. Control*, vol. 50, no. 1, pp. 82–86, Jan. 2005.
[33] W. Michiels and S. Niculescu, "Characterization of delay-independent stability and delay interference phenomena," *SIAM J. Control Optim.*, vol. 45, no. 6, pp. 2138–2155, Jan. 2007.
[34] S.-I. Niculescu, C.-I. Morărescu, W. Michiels, and K. Gu, *Geometric Ideas in the Stability Analysis of Delay Models in Biosciences*. Berlin, Germany: Springer, 2007, pp. 217–259.
[35] R. Sipahi, S.-I. Niculescu, C. T. Abdallah, W. Michiels, and K. Gu, "Stability and stabilization of systems with time delay," *IEEE Control Syst.*, vol. 31, no. 1, pp. 38–65, Feb. 2011.
[36] D. Prousalis and L. Wetzel, "Synchronization in the presence of time delays and inertia: Stability criteria," *Phys. Rev. E, Stat. Phys. Plasmas Fluids Relat. Interdiscip. Top.*, vol. 105, no. 1, Jan. 2022, Art. no. 014210.
[37] Y. Kuramoto, "Cooperative dynamics of oscillator community: A study based on lattice of rings," *Prog. Theor. Phys. Suppl.*, vol. 79, pp. 223–240, 1984.
[38] S. Gupta, A. Campa, and S. Ruffo, "Kuramoto model of synchronization: Equilibrium and nonequilibrium aspects," *J. Stat. Mech., Theory Exp.*, vol. 2014, no. 8, Aug. 2014, Art. no. R08001.
[39] L. Wetzel, D. J. Jörg, A. Pollakis, W. Rave, G. Fettweis, and F. Jülicher, "Self-organized synchronization of digital phase-locked loops with delayed coupling in theory and experiment," *PLoS ONE*, vol. 12, no. 2, pp. 1–21, 2017.
[40] H. Lorentz, A. Einstein, H. Minkowski, H. Weyl, and A. Sommerfeld, *The Principle of Relativity: A Collection of Original Memoirs on the Special and General Theory of Relativity* (Dover Books on Physics and Mathematical Physics). New York, NY, USA: Dover, 1952.
[41] C. M. Will, "Clock synchronization and isotropy of the one-way speed of light," *Phys. Rev. D, Part. Fields*, vol. 45, no. 2, pp. 403–411, Jan. 1992.
[42] R. Best, *Phase-Locked Loops* (Professional Engineering). New York, NY, USA: McGraw-Hill, 2003.
[43] C. Hoyer, D. Prousalis, L. Wetzel, R. Riaz, J. Wagner, F. Jülicher, and F. Ellinger, "Mutual synchronization with 24 GHz oscillators," in *Proc. IEEE Int. Symp. Circuits Syst. (ISCAS)*, May 2021, pp. 1–4.
[44] C. Hoyer, L. Wetzel, D. Prousalis, J. Wagner, F. Jülicher, and F. Ellinger, "Stability analysis of mutually synchronized spatially distributed 24 GHz oscillators," in *Proc. IEEE Int. Instrum. Meas. Technol. Conf. Proc. (IMTC)*, May 2022, pp. 1–6.
[45] C. Hoyer, L. Wetzel, D. Prousalis, J. Wagner, F. Julicher, and F. Ellinger, "Mutual synchronization of spatially distributed 24 GHz oscillators up to distances of 500 m," *IEEE Trans. Circuits Syst. II, Exp. Briefs*, early access, May 20, 2022, doi: 10.1109/TCSII.2022.3176827.
[46] S. J. Mason, "Feedback theory-some properties of signal flow graphs," *Proc. IRE*, vol. 41, no. 9, pp. 1144–1156, Sep. 1953.
[47] W. J. Rugh, *Linear System Theory*, 2nd ed. Upper Saddle River, NJ, USA: Prentice-Hall, 1996.
[48] N. J. Cowan, E. J. Chastain, D. A. Vilhena, J. S. Freudenberg, and C. T. Bergstrom, "Nodal dynamics, not degree distributions, determine the structural controllability of complex networks," *PLoS ONE*, vol. 7, no. 6, pp. 1–5, 2012.
[49] J. M. Hendrickx, M. Gevers, and A. S. Bazanella, "Identifiability of dynamical networks with partial node measurements," *IEEE Trans. Autom. Control*, vol. 64, no. 6, pp. 2240–2253, Jun. 2019.
[50] R. F. Riaz, D. Prousalis, C. Hoyer, J. Wagner, F. Ellinger, F. Jülicher, and L. Wetzel, "Stability and transient dynamics of PLLs in theory and experiments," in *Proc. Eur. Conf. Circuit Theory Design (ECCTD)*, Sep. 2020, pp. 1–4.

[51] F. Gardner, *Phaselock Techniques*, 3rd ed. Hoboken, NJ, USA: Wiley, 2005.
[52] M. G. Earl and S. H. Strogatz, "Synchronization in oscillator networks with delayed coupling: A stability criterion," *Phys. Rev. E, Stat. Phys. Plasmas Fluids Relat. Interdiscip. Top.*, vol. 67, no. 3, Mar. 2003, Art. no. 036204.
[53] V. Kroupa, "Noise properties of PLL systems," *IEEE Trans. Commun.*, vol. COM-30, no. 10, pp. 2244–2252, Oct. 1982.
[54] A. Mehrotra, "Noise analysis of phase-locked loops," *IEEE Trans. Circuits Syst. I, Fundam. Theory Appl.*, vol. 49, no. 9, pp. 1309–1316, Sep. 2002.
[55] B. Schäfer, M. Matthiae, M. Timme, and D. Witthaut, "Decentral smart grid control," *New J. Phys.*, vol. 17, Jan. 2015, Art. no. 015002.
[56] G. A. Leonov, N. V. Kuznetsov, M. V. Yuldashev, and R. V. Yuldashev, "Nonlinear dynamical model of Costas loop and an approach to the analysis of its stability in the large," *Signal Process.*, vol. 108, pp. 124–135, Mar. 2015.
[57] N. V. Kuznetsov, G. A. Leonov, M. V. Yuldashev, and R. V. Yuldashev, "Solution of the Gardner problem on the lock-in range of phase-locked loop," 2017, *arXiv:1705.05013*.
[58] M. V. Blagov, O. A. Kuznetsova, E. V. Kudryashova, N. V. Kuznetsov, T. N. Mokaev, R. N. Mokaev, M. V. Yuldashev, and R. V. Yuldashev, "Hold-in, pull-in and lock-in ranges for phase-locked loop with tangential characteristic of the phase detector," *Proc. Comput. Sci.*, vol. 150, pp. 558–566, Jan. 2019.
[59] J. Asmus, C. L. Müller, and I. F. Sbalzarini, "L_p-adaptation: Simultaneous design centering and robustness estimation of electronic and biological systems," *Sci. Rep.*, vol. 7, no. 1, pp. 1–12, Dec. 2017.
[60] B. Wang, C. Gao, W. L. Chen, J. Miao, X. Zhu, Y. Bai, J. W. Zhang, Y. Y. Feng, T. C. Li, and L. J. Wang, "Precise and continuous time and frequency synchronisation at the 5×10^{-19} accuracy level," *Sci. Rep.*, vol. 2, p. 556, Aug. 2012.
[61] J. C. M. Duncan, "Phase synchronization scheme for very long baseline coherent arrays," Ph.D. dissertation, Univ. Politècnica de Catalunya, Barcelona, Spain, 2012. [Online]. Available: https://ieeexplore.ieee.org/stamp/stamp.jsp?arnumber=9305688
[62] W. Zhou, B. Du, Z. Li, S. Dong, Q. Fan, and Y. Shen, "High-precise frequency measurement and link based on phase group synchronization," in *Proc. IEEE Int. Freq. Control Symp.*, May 2012, pp. 1–4.
[63] G. Interdonato, E. Björnson, H. Quoc Ngo, P. Frenger, and E. G. Larsson, "Ubiquitous cell-free massive MIMO communications," *EURASIP J. Wireless Commun. Netw.*, vol. 2019, no. 1, pp. 1–13, Dec. 2019.
[64] T. Jones, D. Arnold, F. Tuffner, R. Cummings, and K. Lee, "Recent advances in precision clock synchronization protocols for power grid control systems," *Energies*, vol. 14, no. 17, p. 5303, Aug. 2021.
[65] S. Fischer, "Observed time difference of arrival (OTDOA) positioning in 3GPP LTE," *Qualcomm White Paper*, vol. 1, no. 1, pp. 1–62, 2014.
[66] M. Appel, F. Winkler, and B. Meffert, "Phase-based high-precision synchronization for wireless networks using FPGAs," in *Proc. IEEE Int. Symp. Precis. Clock Synchronization Meas., Control, Commun. (ISPCS)*, Sep. 2018, pp. 1–6.
[67] H. Si, B. Wang, F. Wang, Y. Chen, and L. Wang, "Absolute phase synchronization over optical fiber," *Opt. Exp.*, vol. 28, no. 4, pp. 4603–4610, Feb. 2020.
[68] B. Sonnenschein and L. Schimansky-Geier, "Onset of synchronization in complex networks of noisy oscillators," *Phys. Rev. E, Stat. Phys. Plasmas Fluids Relat. Interdiscip. Top.*, vol. 85, no. 5, May 2012, Art. no. 051116.

LUCAS WETZEL received the joint Diploma degree in physics from Leipzig University and ETH Zürich, in 2008, and the Ph.D. degree in physics from the Max Planck Institute for the Physics of Complex Systems, TU Dresden (TUD), Dresden, in 2012. During his Diploma studies, he specialized on micro- and nanosystems, stochastic processes, and nonlinear dynamics. He has supervised his Diploma thesis on the statistical properties of stochastic delay differential equations with additive and multiplicative noise. Since 2008, he has been with the Max Planck Institute for the Physics of Complex Systems, Dresden. In the following, he arranged a collaboration with the Vodafone Chair Mobile Communications Systems, TUD; and within the Center for Advancing Electronics Dresden, studying mutual synchronization inspired from biological systems and its application to electronic systems. In 2019, he received together with the Chair of Circuit Design and Network Theory, TUD; and the Fraunhofer Institute for Reliability and Microintegration IZM, Dresden, a VIP+ grant from the German Federal Ministry of Education and Research to validate mutual networks synchronization. His research interests include nonlinear dynamics in systems with time-delayed interactions and control theoretical approaches to nonlinear systems with the goal to advance ideas from basic research to application. He is a member of the German Physical Society DPG.

DIMITRIOS PROUSALIS received the B.Sc. and M.Sc. degrees in physics, specializing in theoretical physics with strong interest in nonlinear dynamics and chaos, and the Ph.D. degree in theoretical physics from the Aristotle University of Thessaloniki. During his Ph.D. degree, he focused on the dynamics of memristive systems and circuits. Following his Ph.D. degree, he joined as a Postdoctoral Researcher at the Max Planck Institute for the Physics of Complex System, Dresden, Germany, to work on emergent phenomena in networks of delay-coupled oscillators. His research interests include the fields of stochastic and chaotic dynamics of systems and circuits, particularly the synchronization of coupled oscillators and applying the theory of dynamical systems to engineering applications.

RABIA FATIMA RIAZ was born in Lahore, Pakistan, in June 1991. She received the bachelor's degree in electrical engineering (science) from the Lahore University of Management Sciences, in June 2014, and the master's degree in nanoelecteonics from Technische Universität Dresden, in March 2019. Since then, she has been employed as a Scientific Researcher with the Chair of Circuit Design and Network Theory, Technische Universität Dresden. Her research interests include control systems theory, analog circuit design, feedback systems, phase locked loops, and integrated circuit design.

CHRISTIAN HOYER was born in 1992. He received the B.Sc. degree in electrical engineering from the University of Kassel, in 2017, and the M.Sc. degree in electrical engineering, with a specialty in high-frequency electronics, from the Karlsruhe Institute of Technology, in 2019. He is currently pursuing the Ph.D. degree in high-frequency analog integrated circuits with the Chair of Circuit Design and Network Theory, Technische Universität Dresden, Germany. During his studies, he was working for several research and development projects in industry and research institutions. His master's thesis was done at the Fraunhofer Institute for Applied Solid State Physics IAF, Freiburg im Breisgau, in the research field of wideband GaN high power amplifiers. His research interests include high-precision synchronization, high-frequency integrated circuits, and oscillators.

NIKO JORAM was born in Oelsnitz, Germany, in 1984. He received the Ph.D. degree in electrical engineering from Technische Universität Dresden. He is currently leading the Local Positioning and Radar Research Group, Chair for Circuit Design and Network Theory. His research interests include circuit and systems design for robust localization and radar systems.

JOHANNES FRITZSCHE was an IT-Systems Electronics Technician, in 1994, and has an additional socio-psychiatric qualification, in 2011. He gained experience inspecting memory and ASIC components, from 1985 to 1991, at the Measuring Technology Department of a semiconductor manufacturer in Dresden, Germany. He is currently a Group Leader in a social enterprise. He uses electronics production as a tool for health-oriented labor promotion. He has long-standing experience as a Media Educator and a Studio Engineer working for an educational radio station. He is involved in bringing together the arts and sciences using his electronic prototyping skills with independent developers, artists, and within groups, such as KAZOOSH! He has been captivated by electronic circuits since early childhood and has been continuously improving upon his skills in this field. He has also been working on hardware-near programming of microcontrollers and circuit simulation in his private working space.

FRANK ELLINGER (Senior Member, IEEE) received the degree in electrical engineering (EE) from the University of Ulm, Germany, in 1996, the post-graduation Diploma degree in business and administration from ETH Zürich (ETHZ), Switzerland, in 2001, and the Ph.D. and Habilitation degrees in EE from ETHZ, in 2001 and 2005, respectively. From 2001 to 2006, he was the Head of the Electronics Laboratory, RFIC Design Group, ETHZ; and the Project Leader of the IBM/ETHZ Competence Center for Advanced Silicon Electronics hosted at IBM Research, Rüschlikon. Since August 2006, he has been a Full Professor and the Head of the Chair for Circuit Design and Network Theory, Technische Universität Dresden, Germany. He coordinates the BMBF Cluster Project FAST and the DFG Priority Program FFlexCom. As an author and a coauthor, he has published more than 500 scientific papers. He has received several awards, such as the Vodafone Innovation Award, the Alcatel Lucent Science Award, and the IEEE Outstanding Young Engineer Award, and was an IEEE Distinguished Lecturer.

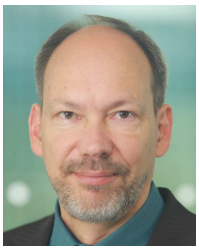

FRANK JÜLICHER received the Ph.D. degree from the University of Cologne, in 1994, under the supervision of Prof. Reinhard Lipowsky, and the Habilitation degree from the University of Paris VII, in 2000. Following his postdoctoral research at Simon Fraser University, Canada; the Institut Curie, Paris; and ESPCI, France, he was appointed at the Institut Curie with a CNRS research position, in 1998. Since 2002, he has been the Director of the Max Planck Institute for the Physics of Complex Systems, Dresden, Germany; and a Professor in biophysics with TU Dresden. His research interests include theoretical approaches to dynamic processes in cells and tissues, which include active cellular processes, such as cellular oscillations, cell division, and collective phenomena, including tissue morphogenesis. He received the Robert Wichard Pohl Prize of the DPG, the Raymond and Beverly Sackler International Prize in Biophysics, and the Gottfried Wilhelm Leibniz Price.